

RESULTADOS RECENTES SOBRE ENTROPIA NÃO ADITIVA E MECÂNICA ESTATÍSTICA NÃO EXTENSIVA

Constantino Tsallis

Centro Brasileiro de Pesquisas Físicas

e Instituto Nacional de Ciência e Tecnologia de Sistemas Complexos

Rio de Janeiro

e

Santa Fe Institute, New Mexico

INCT-SC, Rio de Janeiro, Março 2010

EVIDÊNCIAS E APLICAÇÕES RECENTES:

Spin-glass

Multiple sclerosis magnetic resonance images

Interstellar turbulence

Quantum entangled spin-S chains

Ozone layer

X-ray binary systems

Seismic sequences

Motion of *Dictyostelium discoideum* (cells)

Periodic map edge of chaos

SOC in coherent noise model

LHC (CMS detector)

QUESTÕES TEÓRICAS EM CURSO:

Physical characterization of q -independence

Possibility of simultaneous $q_{entropy} \neq 1$ and $q_{limit} \neq 1$

SPIN RELAXATION IN SPIN GLASSES (NEUTRON SPIN ECHO):

PRL 102, 097202 (2009)

PHYSICAL REVIEW LETTERS

week ending
6 MARCH 2009

Generalized Spin-Glass Relaxation

R. M. Pickup,¹ R. Cywinski,^{2,*} C. Pappas,³ B. Farago,⁴ and P. Fouquet⁴

¹*School of Physics and Astronomy, University of Leeds, Leeds LS2 9JT, United Kingdom*

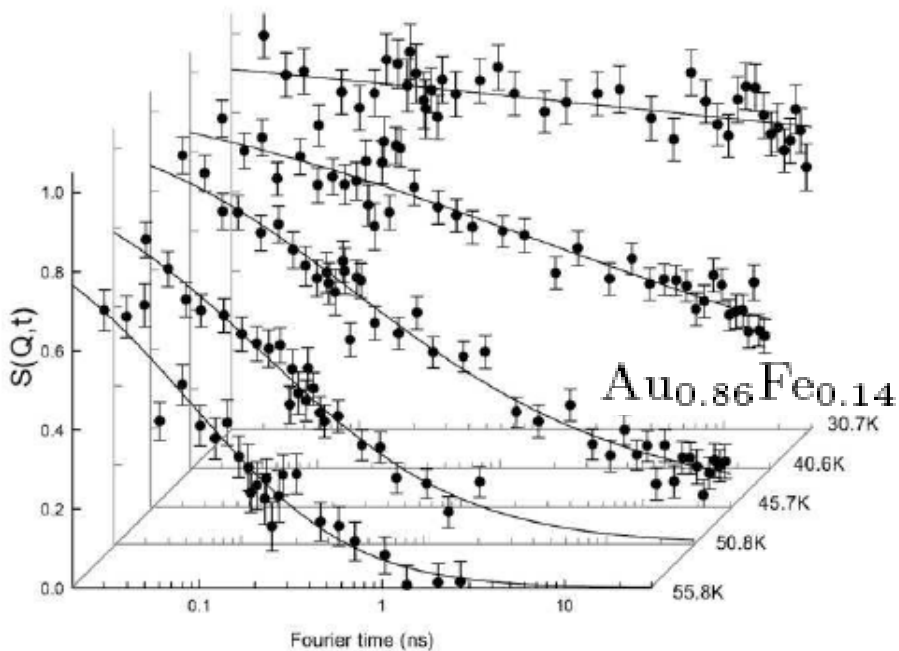
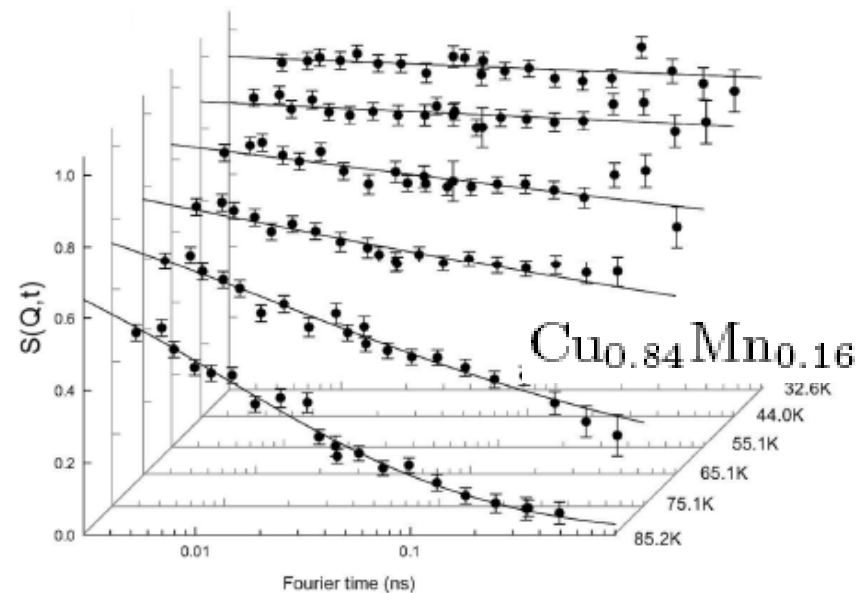
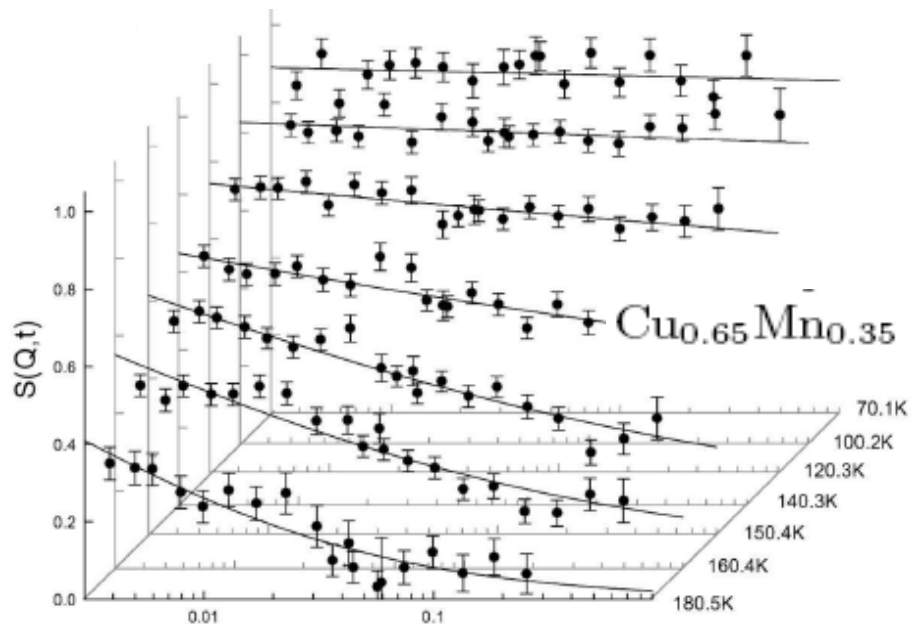
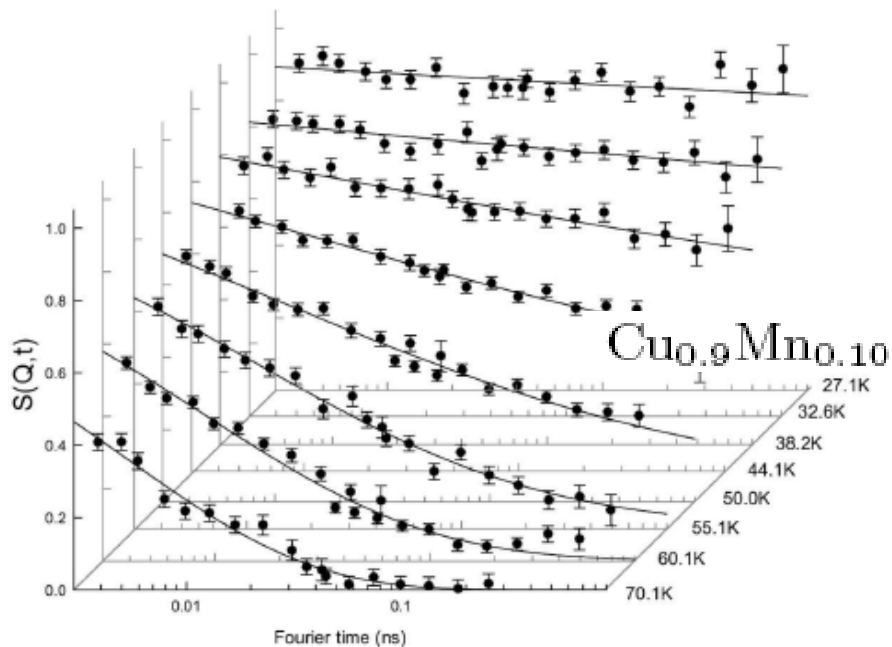
²*School of Applied Sciences, University of Huddersfield, Huddersfield HD1 3DH, United Kingdom*

³*Helmholtz Center Berlin for Materials and Energy, Glienickerstrasse 100, 14109, Berlin, Germany*

⁴*Institut Laue Langevin, 6 rue Jules Horowitz, 38000 Grenoble, France*

(Received 18 July 2008; published 4 March 2009)

Spin relaxation close to the glass temperature of CuMn and AuFe spin glasses is shown, by neutron spin echo, to follow a generalized exponential function which explicitly introduces hierarchically constrained dynamics and macroscopic interactions. The interaction parameter is directly related to the normalized Tsallis nonextensive entropy parameter q and exhibits universal scaling with reduced temperature. At the glass temperature $q = 5/3$ corresponding, within Tsallis' q statistics, to a mathematically defined critical value for the onset of strong disorder and nonlinear dynamics.

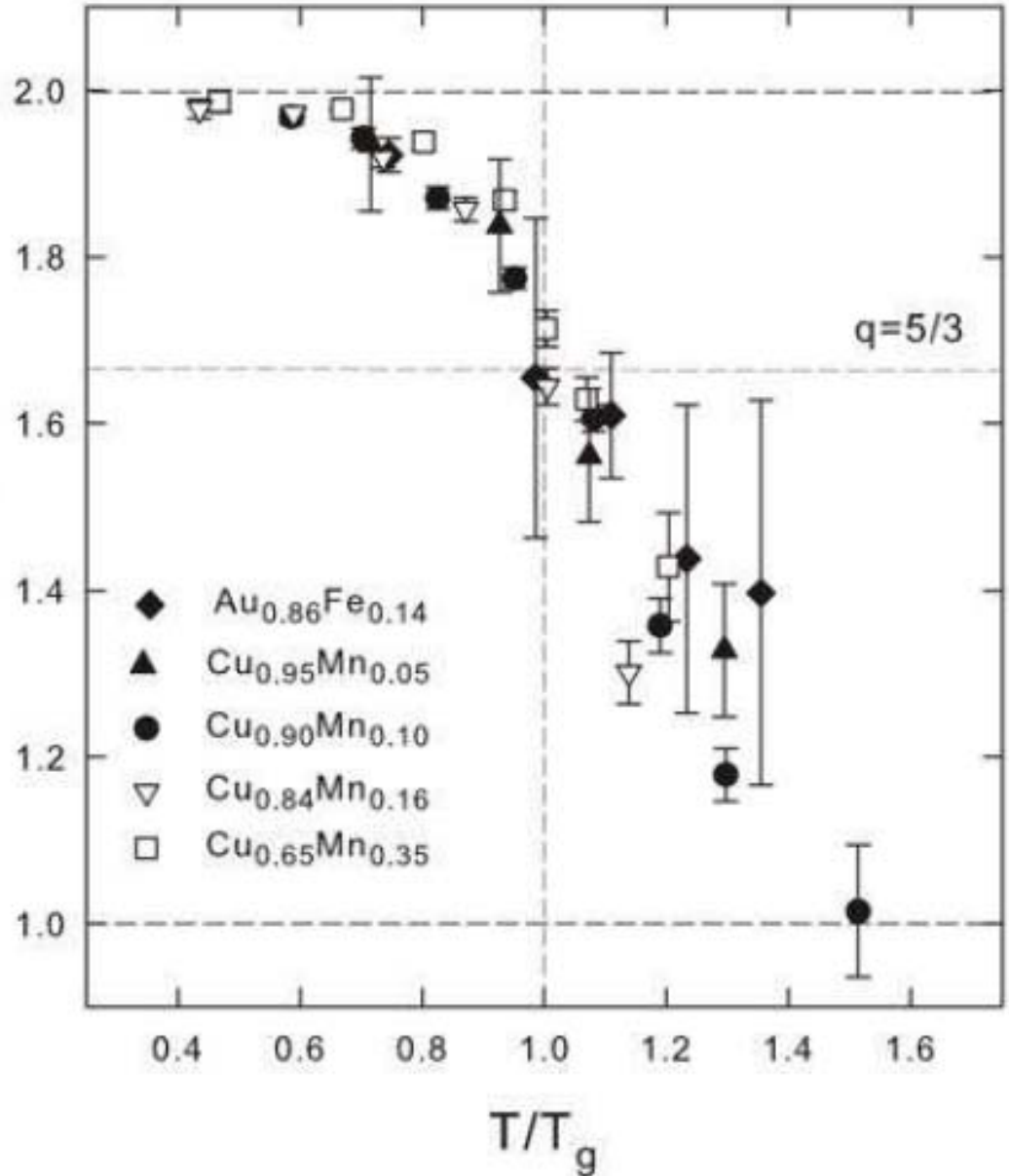


SPIN RELAXATION IN SPIN GLASSES (NEUTRON SPIN ECHO):

$$\phi(t) = \left[1 + \frac{q-1}{2-q} \left(\frac{t}{\tau} \right)^\beta \right]^{-\frac{2-q}{q-1}}$$

$$\equiv \left[1 + (q_{rel} - 1) \left(\frac{t}{\tau} \right)^\beta \right]^{-\frac{1}{q_{rel}-1}}$$

$$q_{rel} \equiv \frac{1}{2-q}$$



Brain tissue segmentation using q-entropy in multiple sclerosis magnetic resonance images

P.R.B. Diniz¹, L.O. Murta-Junior³, D.G. Brum¹, D.B. de Araújo³ and A.C. Santos^{1,2}

¹Departamento de Neurociências e Ciências do Comportamento, ²Departamento de Clínica Médica, Divisão de Radiologia, Faculdade de Medicina de Ribeirão Preto, Universidade de São Paulo, Ribeirão Preto, SP, Brasil

³Departamento de Física e Matemática, Faculdade de Filosofia, Ciências e Letras de Ribeirão Preto, Universidade de São Paulo, Ribeirão Preto, SP, Brasil

Abstract

The loss of brain volume has been used as a marker of tissue destruction and can be used as an index of the progression of neurodegenerative diseases, such as multiple sclerosis. In the present study, we tested a new method for tissue segmentation based on pixel intensity threshold using generalized Tsallis entropy to determine a statistical segmentation parameter for each single class of brain tissue. We compared the performance of this method using a range of different q parameters and found a different optimal q parameter for white matter, gray matter, and cerebrospinal fluid. Our results support the conclusion that the differences in structural correlations and scale invariant similarities present in each tissue class can be accessed by generalized Tsallis entropy, obtaining the intensity limits for these tissue class separations. In order to test this method, we used it for analysis of brain magnetic resonance images of 43 patients and 10 healthy controls matched for gender and age. The values found for the entropic q index were 0.2 for cerebrospinal fluid, 0.1 for white matter and 1.5 for gray matter. With this algorithm, we could detect an annual loss of 0.98% for the patients, in agreement with literature data. Thus, we can conclude that the entropy of Tsallis adds advantages to the process of automatic target segmentation of tissue classes, which had not been demonstrated previously.

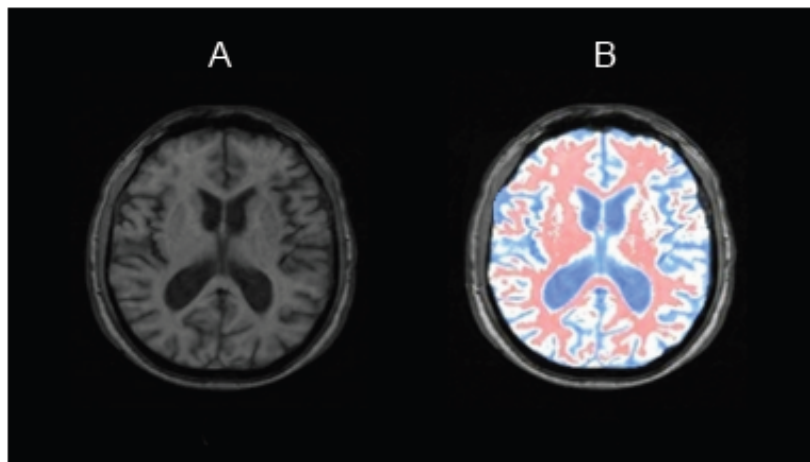


Figure 3. Maximum entropy segmentation example. A, Original image; B, image with the segmentation masks. Blue indicates cerebrospinal fluid, white indicates the gray matter, and red indicates the white matter.

The ideal q values for the segmentation of the classes are: CSF = 0.2, WM = 0.1, GM = 1.5, which have not been shown previously.

These characteristics allow its application to clinical routine.

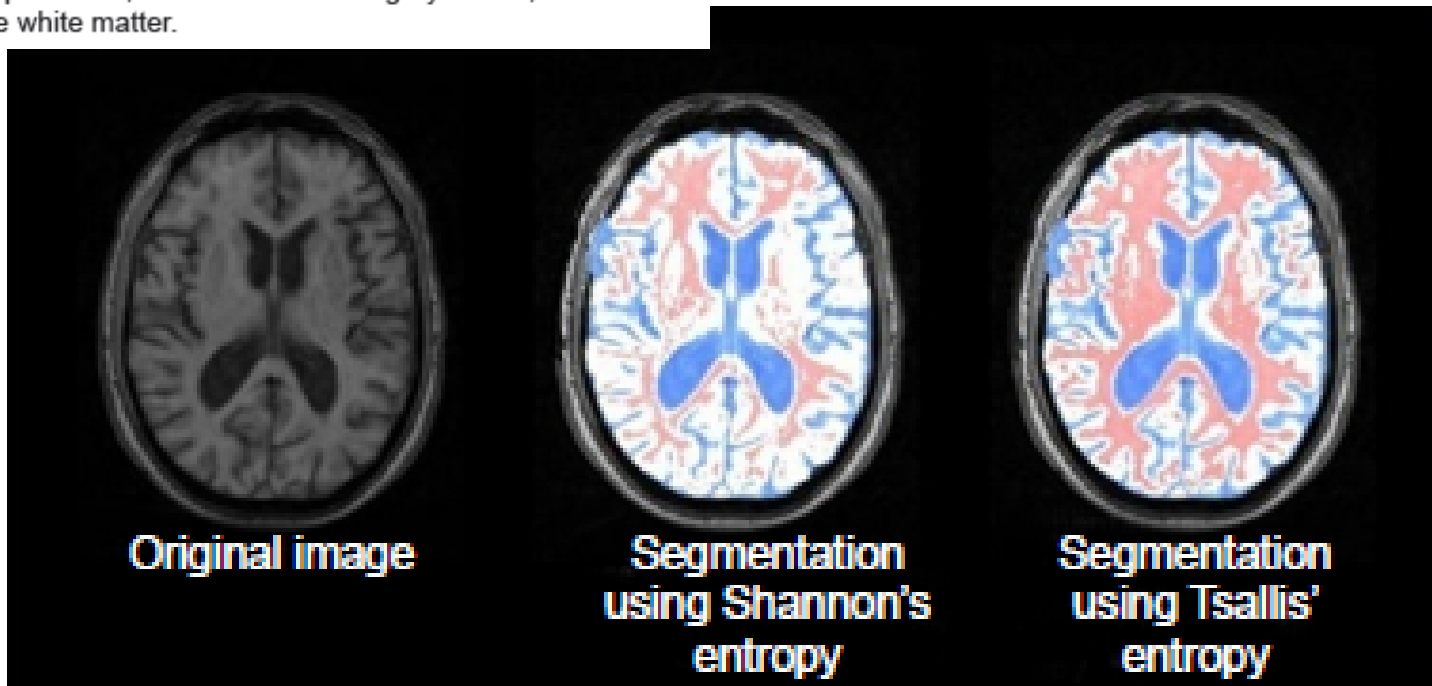


Figure 6. Segmentation using Shannon and Tsallis entropies.

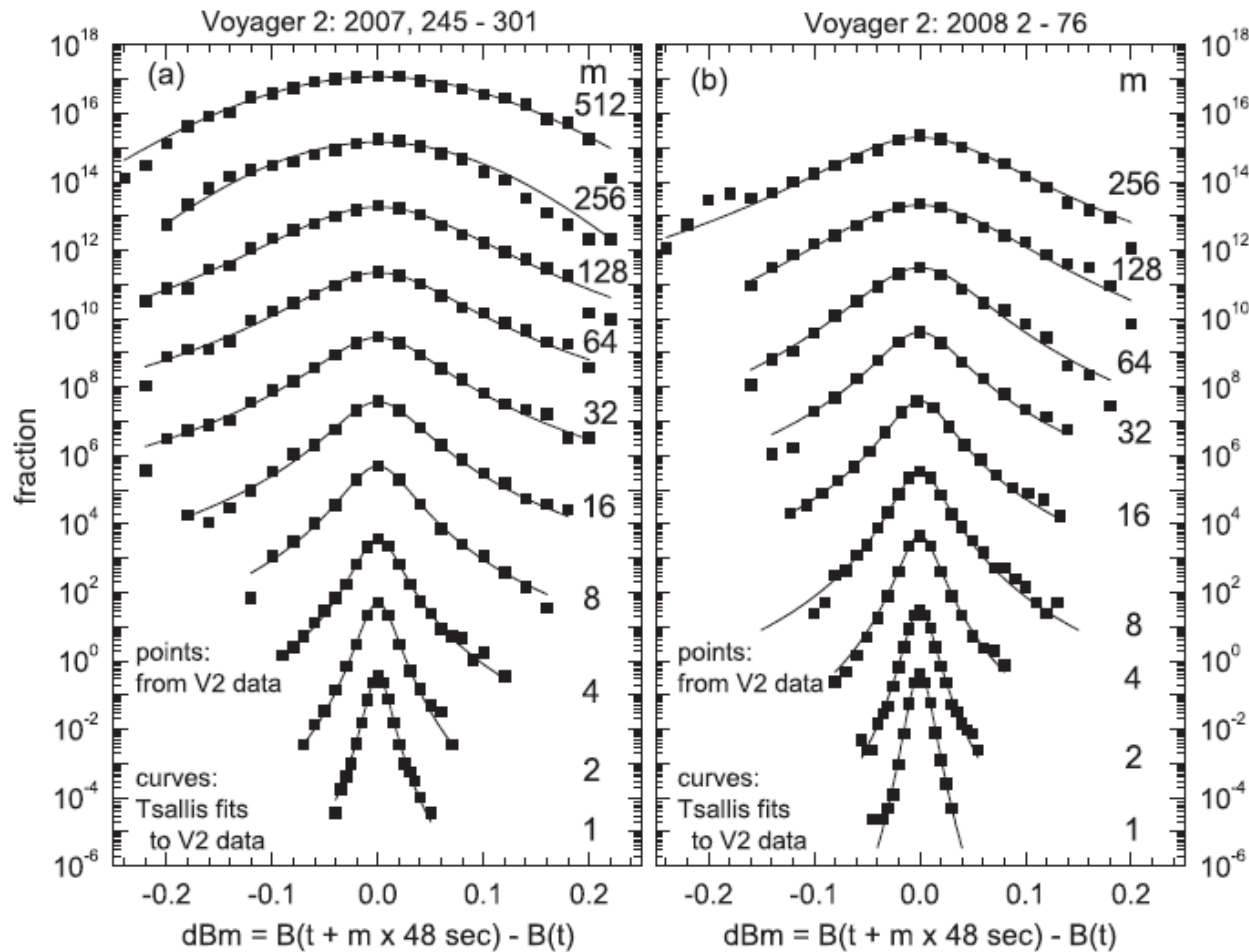
COMPRESSIBLE “TURBULENCE” OBSERVED IN THE HELIOSHEATH BY *VOYAGER 2*

L. F. BURLAGA¹ AND N. F. NESS²

¹ Geospace Physics Laboratory, Code 673, NASA Goddard Space Flight Center, Greenbelt, MD 20771, USA; Leonard.F.Burlaga@NASA.gov

² Institute for Astrophysics and Computational Sciences, Catholic University of America, Washington DC 20064, USA; nfnudel@yahoo.com

Received 2009 June 2; accepted 2009 July 22; published 2009 August 27



TSALLIS STATISTICS AS A TOOL FOR STUDYING INTERSTELLAR TURBULENCE

A. ESQUIVEL¹ AND A. LAZARIAN²

¹ Instituto de Ciencias Nucleares, Universidad Nacional Autónoma de México, Apartado Postal 70-543, 04510 México D.F., México; esquivel@nucleares.unam.mx

² Astronomy Department, University of Wisconsin-Madison, 475 N. Charter Street, Madison, WI 53706-1582, USA; lazarian@astro.wisc.edu

Received 2009 May 15; accepted 2009 December 15; published 2010 January 15

ABSTRACT

We used magnetohydrodynamic (MHD) simulations of interstellar turbulence to study the probability distribution functions (PDFs) of increments of density, velocity, and magnetic field. We found that the PDFs are well described by a Tsallis distribution, following the same general trends found in solar wind and electron MHD studies. We found that the PDFs of density are very different in subsonic and supersonic turbulence. In order to extend this work to ISM observations, we studied maps of column density obtained from three-dimensional MHD simulations. From the column density maps, we found the parameters that fit to Tsallis distributions and demonstrated that these parameters vary with the sonic and Alfvén Mach numbers of turbulence. This opens avenues for using Tsallis distributions to study the dynamical and perhaps magnetic states of interstellar gas.

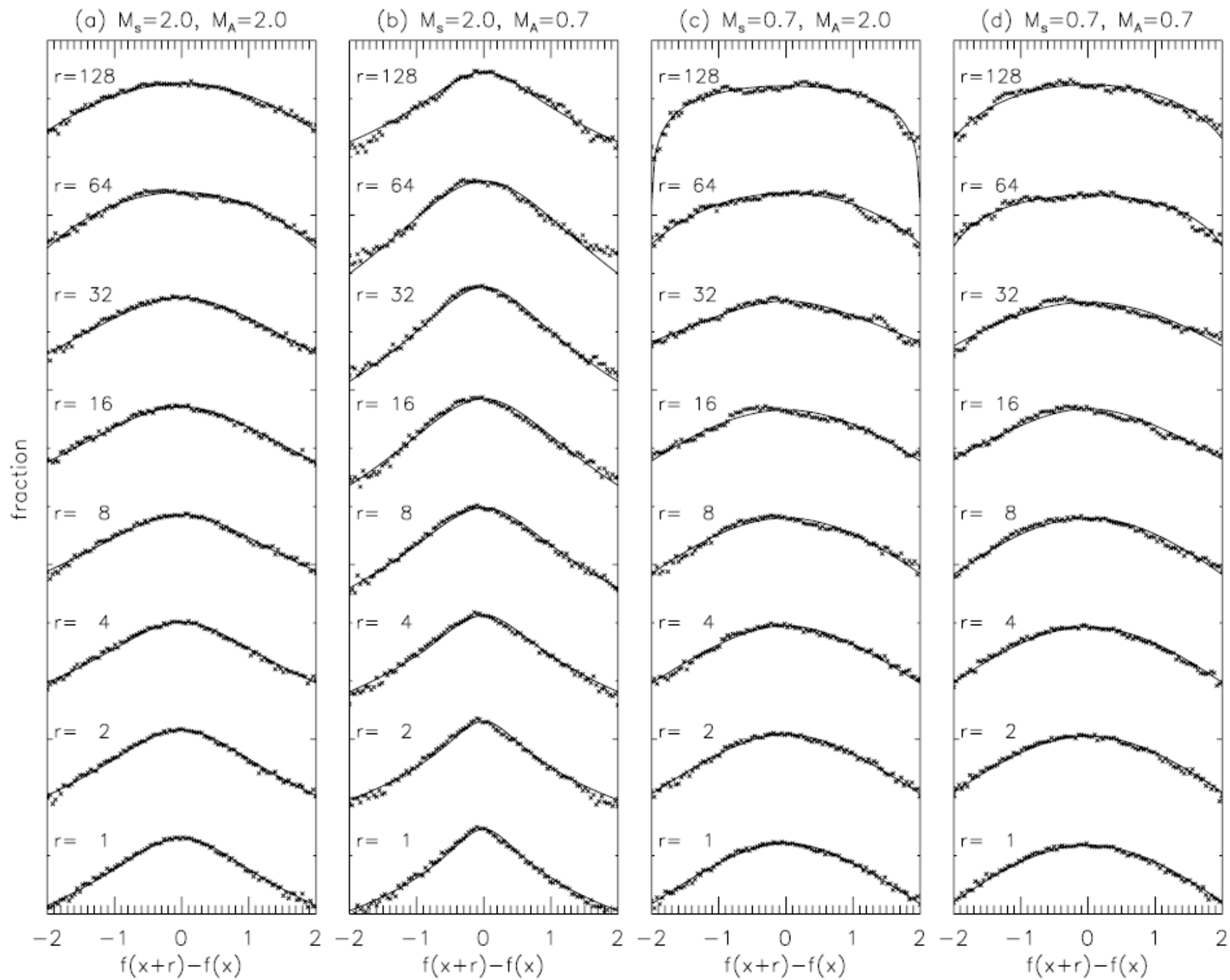


Figure 4. PDFs of column density fluctuations for different spatial separations (“x” symbols) and Tsallis fits (solid lines).

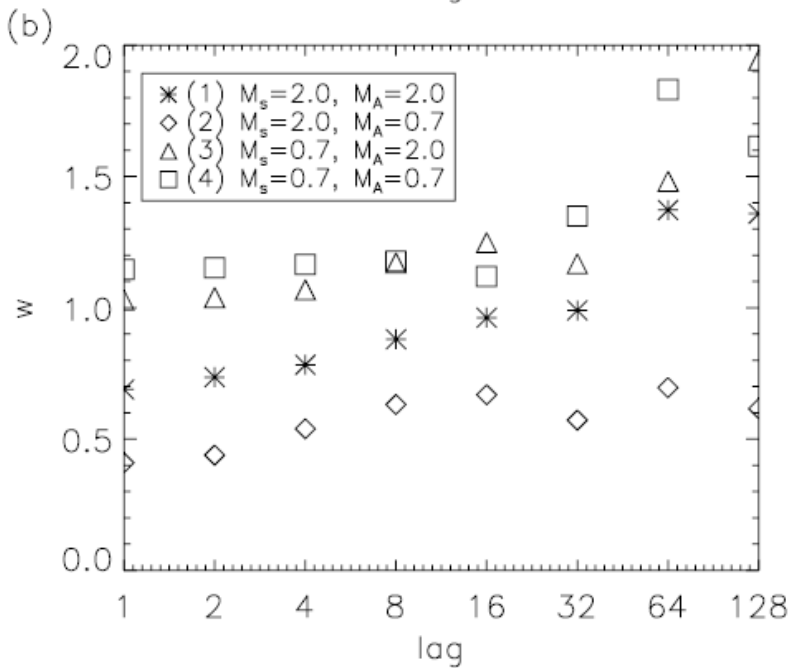
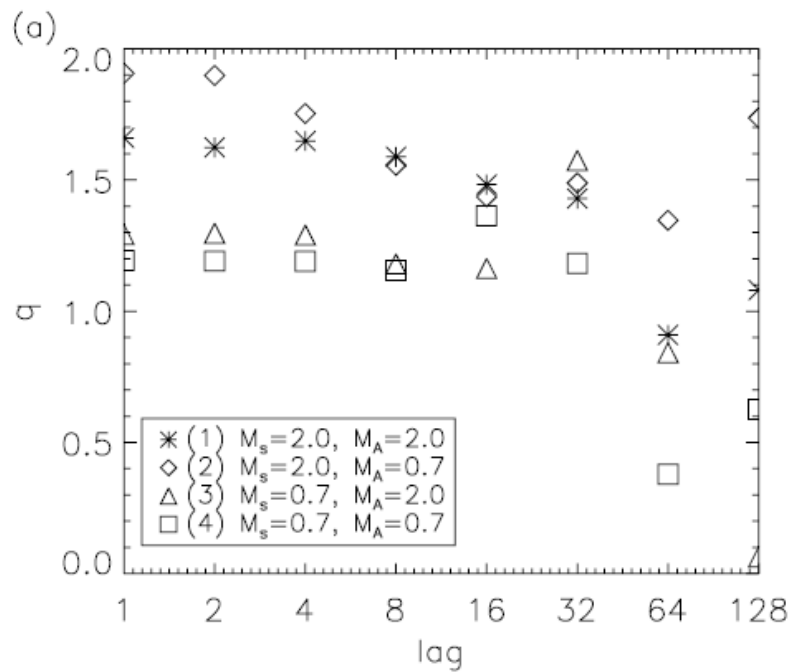


Figure 5. Parameters q and w from d , the Tsallis distribution fits shown in Figure 4.

A. Esquivel and A. Lazarian
 Astrophys. J. **710**, 125 (2010)



Contents lists available at ScienceDirect

Physica A

journal homepage: www.elsevier.com/locate/physa



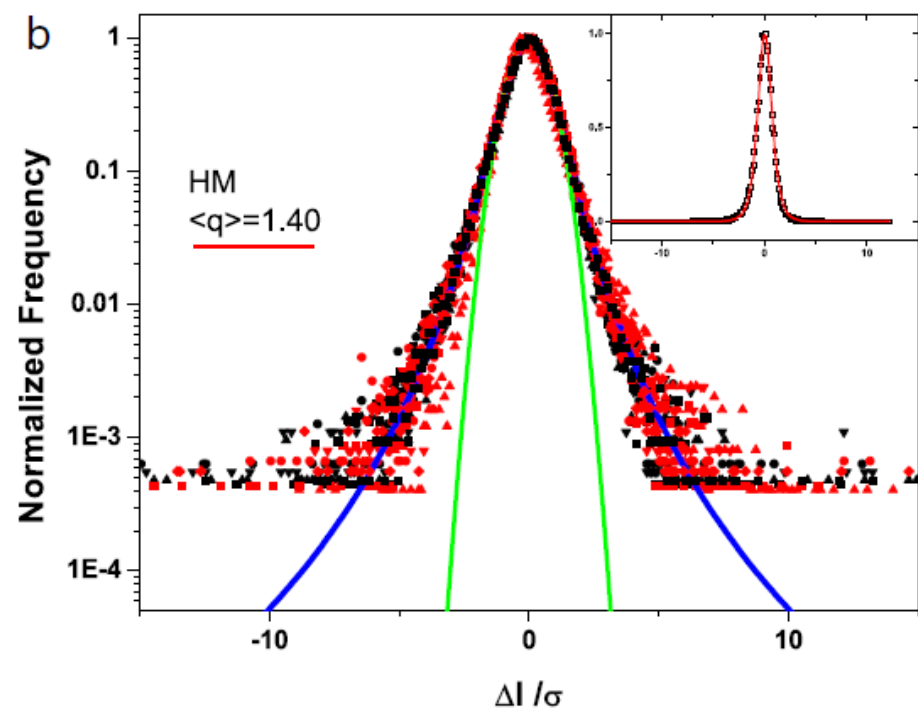
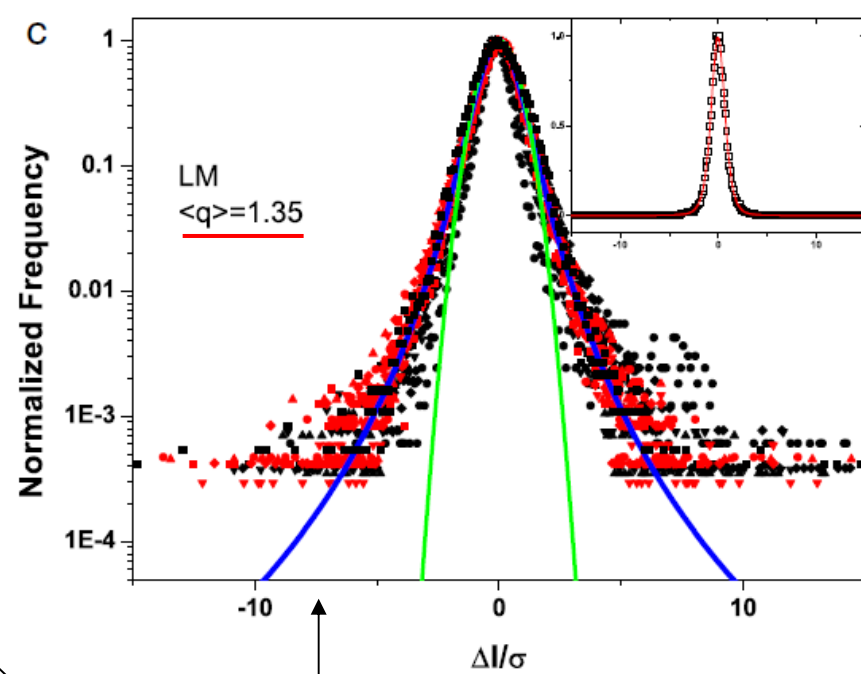
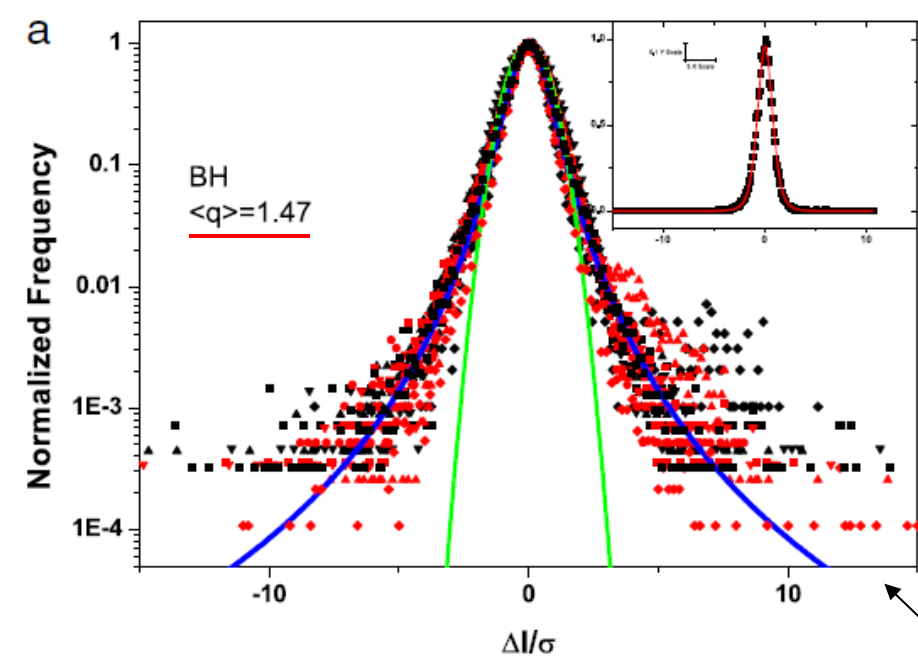
X-ray binary systems and nonextensivity

Marcelo A. Moret^{a,b,*}, Valter de Senna^a, Gilney F. Zebende^{a,b}, Pablo Vaveliuk^a

^a Programa de Modelagem Computacional - SENAI - CIMATEC 41650-010 Salvador, Bahia, Brazil

^b Departamento de Física, Universidade Estadual de Feira de Santana, CEP 44031-460, Feira de Santana, Bahia, Brazil

Distributions of intensities of X-ray emission



Low mass neutron stars

Black hole candidates

High mass neutron stars

Nonadditive entropy for random quantum spin-S chains

A. Saguia* and M. S. Sarandy†

Instituto de Física, Universidade Federal Fluminense,

Av. Gal. Milton Tavares de Souza s/n, Gragoatá, 24210-346, Niterói, RJ, Brazil.

(Dated: December 21, 2009)

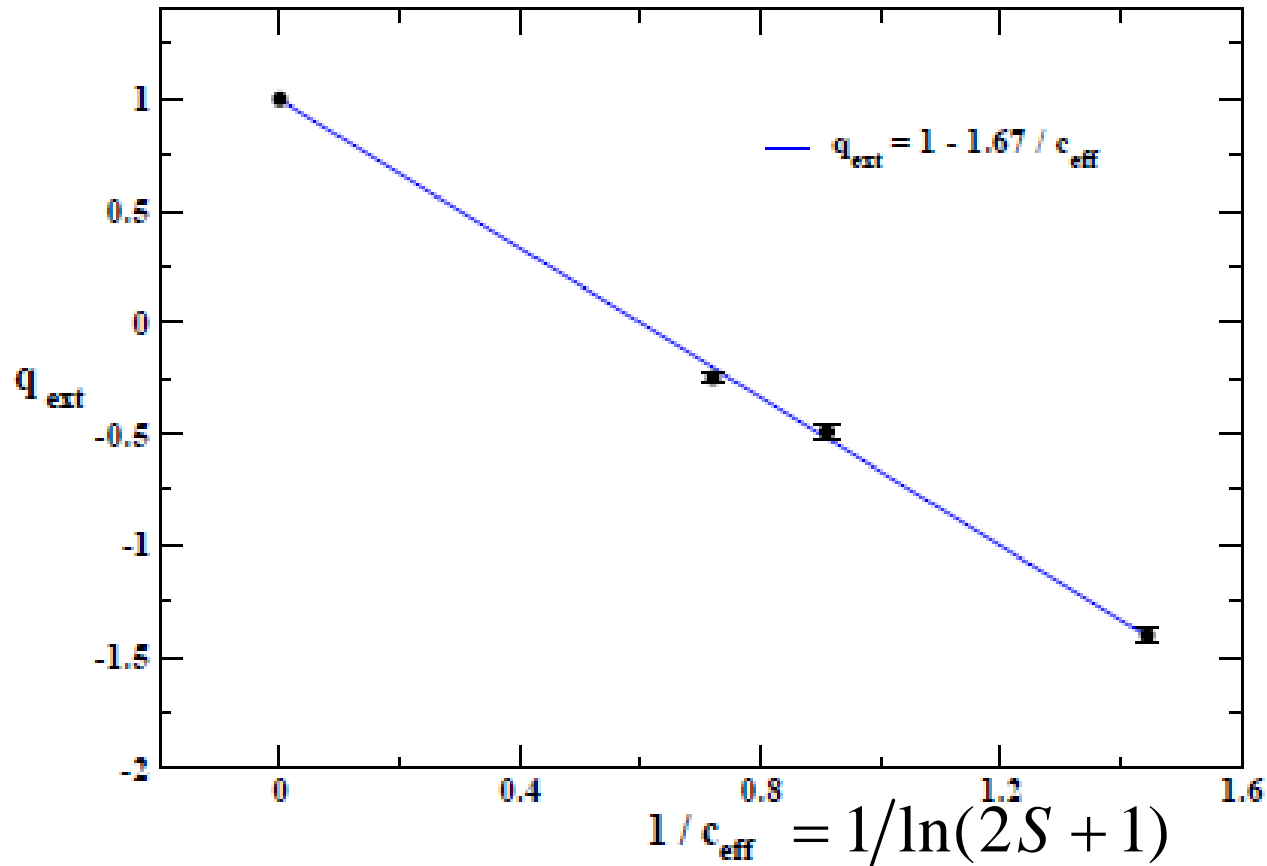


FIG. 7: (Color online) Extensivity index q_{ext} as a function of the effective central charge c_{eff} for REHACs in the RSP.



Contents lists available at ScienceDirect

Physica A

journal homepage: www.elsevier.com/locate/physa



Tsallis' q -triplet and the ozone layer

G.L. Ferri^{a,*}, M.F. Reynoso Savio^a, A. Plastino^b

^a *Facultad de Ciencias Exactas, Universidad Nacional de La Pampa, Peru y Uruguay, 6300, Santa Rosa, La Pampa, Argentina*

^b *La Plata Physics Institute, Exact Sciences Fac., National University of La Plata, Argentina's National Research Council (CCT-CONICET), C.C. 727, (1900) La Plata, Argentina*

ARTICLE INFO

Article history:

Received 23 September 2009

Received in revised form 24 November 2009

Available online 22 December 2009

ABSTRACT

Tsallis' q -triplet [C. Tsallis, Dynamical scenario for nonextensive statistical mechanics, *Physica A* 340 (2004) 1–10] is the best empirical quantifier of nonextensivity. Here we study it with reference to an experimental time-series related to the daily depth-values of the stratospheric ozone layer. Pertinent data are expressed in Dobson units and range from 1978 to 2005. After the evaluation of the three associated Tsallis' indices one concludes that nonextensivity is clearly a characteristic of the system under scrutiny.

Original data = mean value + long range tendency + annual oscillation + quasi-biannual one + Z_n

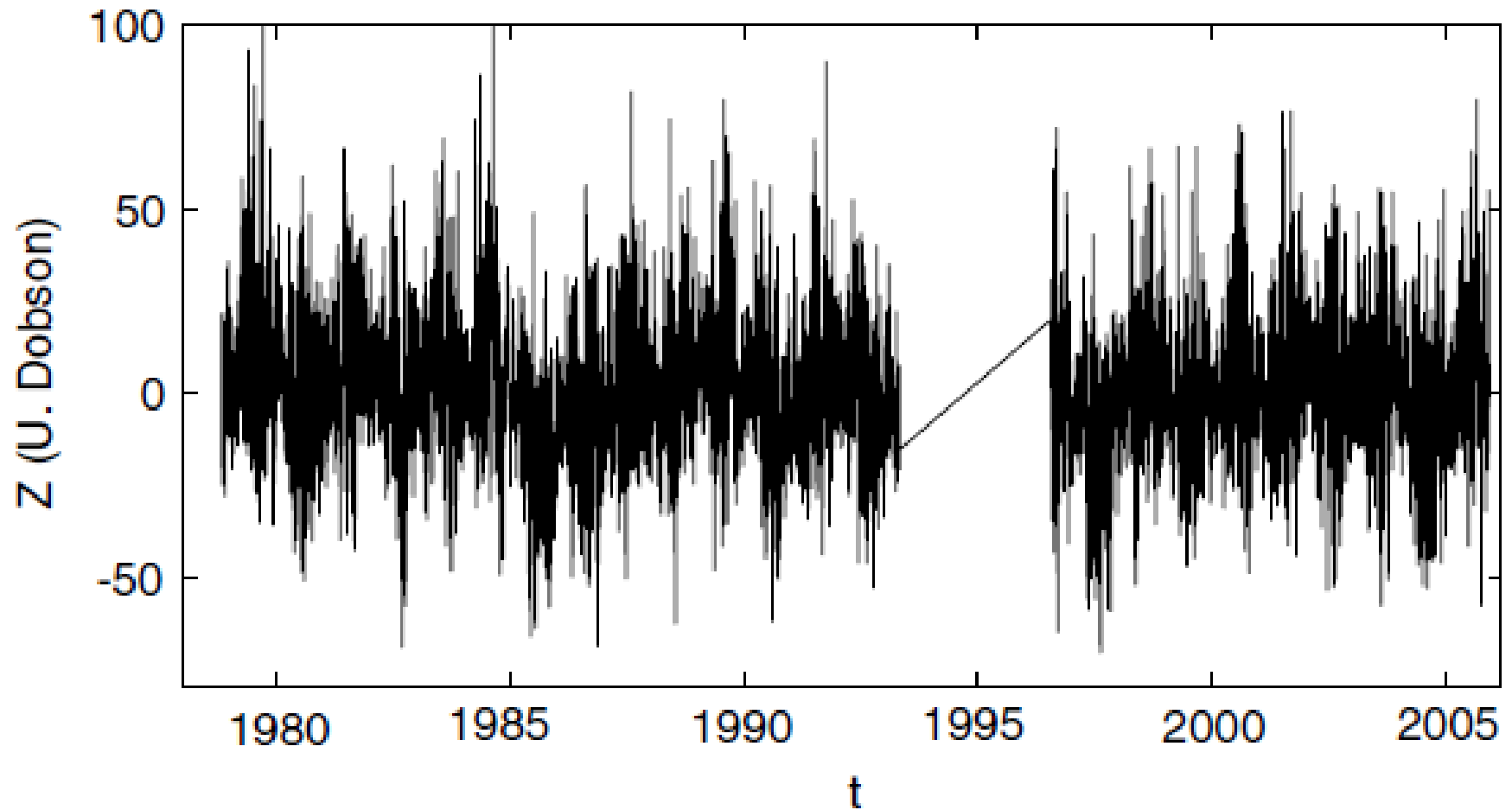


Fig. 1. Time-series Z_n . Daily values of the ozone layer over Buenos Aires city.

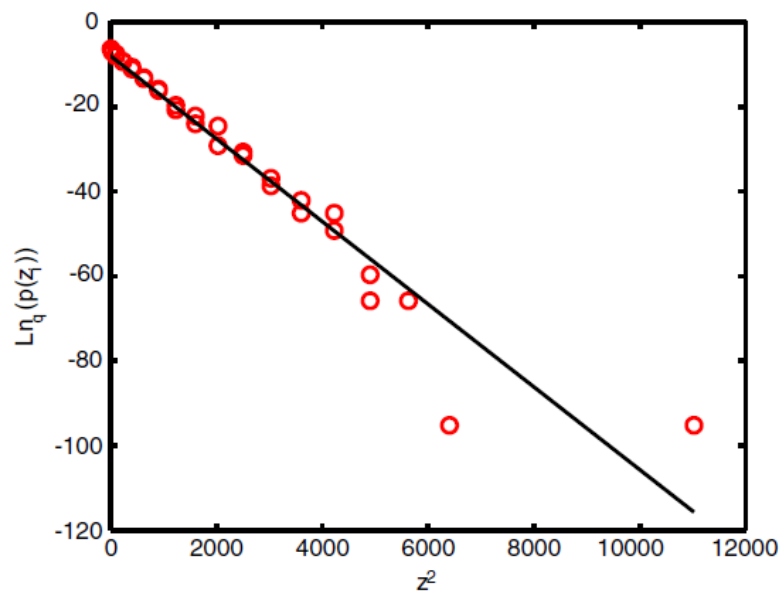


Fig. 2. Linear correlation between $\ln_q[p(z_i)]$ and z_i^2 , where $q_{\text{stat}} = 1.32 \pm 0.06$. The linear CC. is 0.9383.

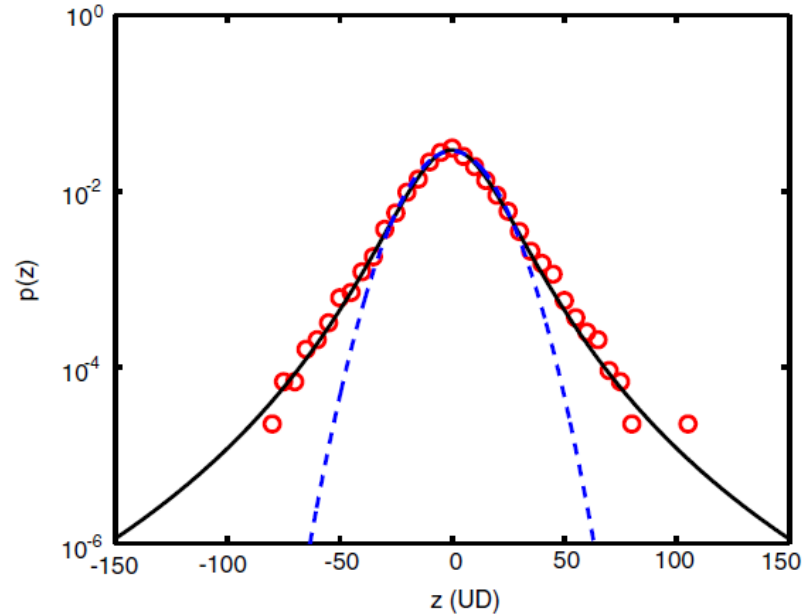


Fig. 3. In red circles, $p(z_i)$ vs. z_i ; in solid black line, the q -Gaussian function that fits $p(z_i)$, Eq. (3), with $\beta = 0.00356$; in dashed blue line, the best adjustment with a *Gaussian*. (For interpretation of the references to colour in this figure legend, the reader is referred to the web version of this article.)

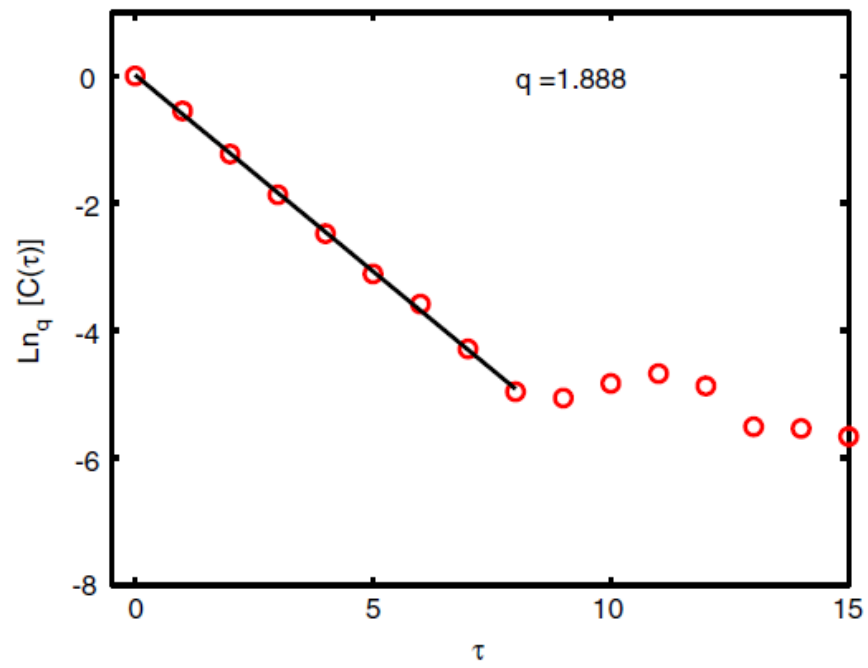


Fig. 4. Ln_q of the self-correlation coefficient $C(\tau)$ vs. time delay τ (in days). We obtain the best fit with $q_{\text{rel}} = 1.888$. The linear CC is 0.99919.

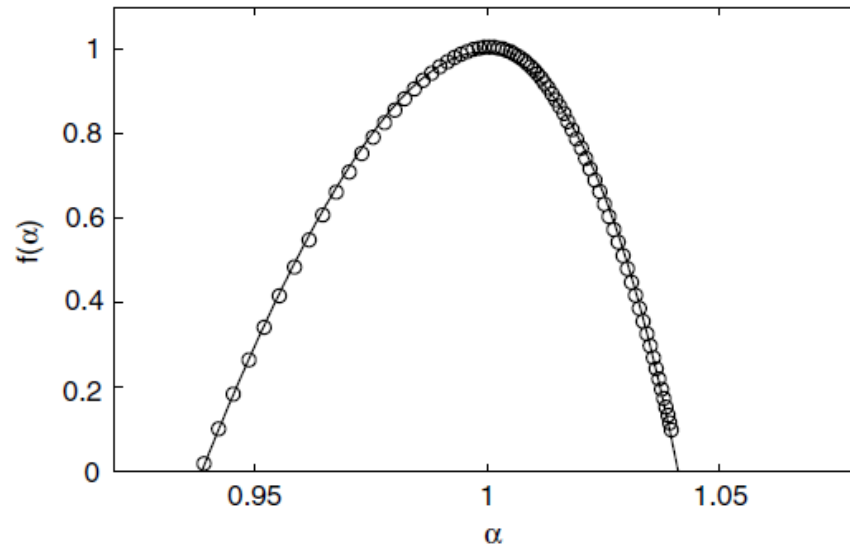


Fig. 5. Multifractal spectrum of ozone time series. $\alpha_{\text{min}} = 0.938 \pm 0.001$ and $\alpha_{\text{max}} = 1.046 \pm 0.001$.

$$q_{stat} = 1.32 \pm 0.06$$

$$q_{sens} = -8.1 \pm 0.02$$

$$q_{rel} = 1.89 \pm 0.02$$

hence

$$q_{sens} < 1 < q_{stat} < q_{rel}$$

EDGE OF CHAOS OF THE LOGISTIC MAP:

$$q\text{-triplet} \left\{ \begin{array}{l} q_{sensitivity} = q_{entropy} = 0.244487701341282066198\dots \\ q_{relaxation} = 2.249784109\dots \\ q_{stationary\ state} = 1.65 \pm 0.05 \end{array} \right.$$

hence

$$q_{sens} < 1 < q_{stat} < q_{rel}$$



Contents lists available at ScienceDirect

Physica A

journal homepage: www.elsevier.com/locate/physa



Nonextensive analysis of seismic sequences

Luciano Telesca

Istituto di Metodologie per l'Analisi Ambientale, CNR, C.da S.Loja, 85050 Tito (PZ), Italy

ARTICLE INFO

Article history:

Received 6 November 2009

Received in revised form 18 December 2009

Available online 16 January 2010

Keywords:

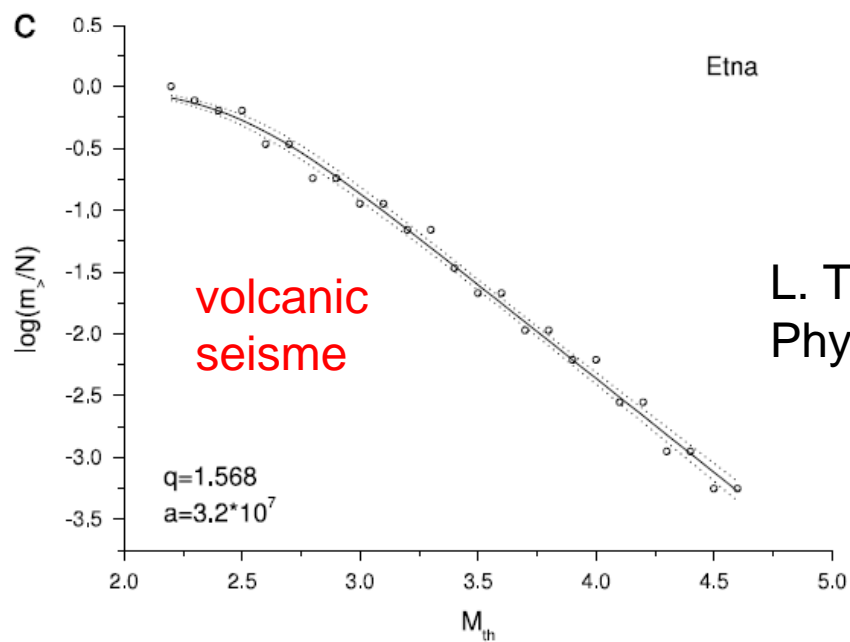
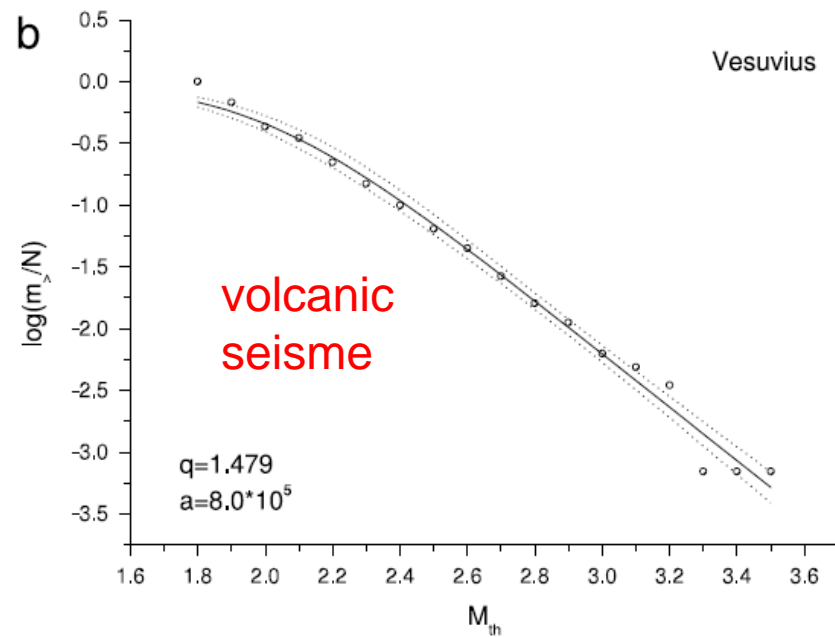
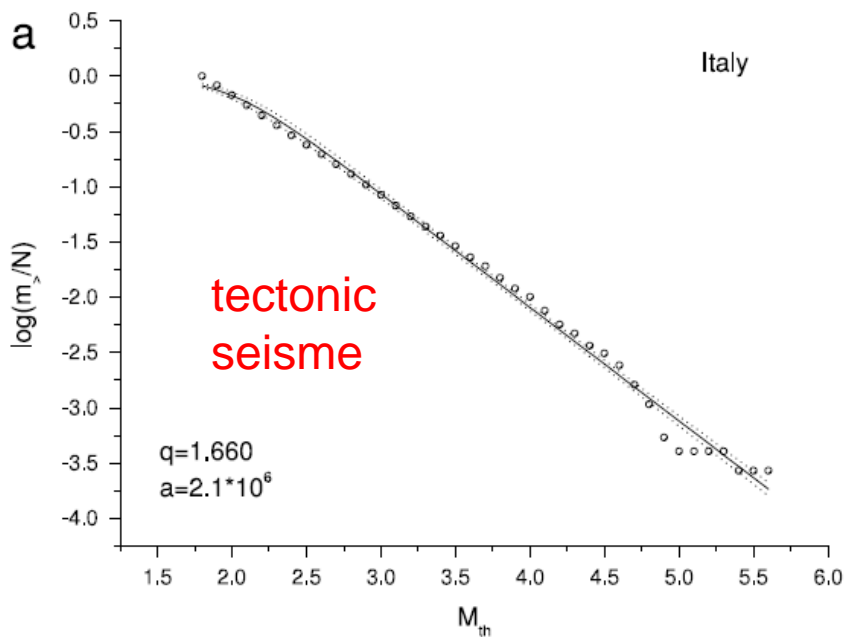
Nonextensive statistics

Earthquakes

ABSTRACT

By using the Tsallis-based nonextensive statistics, the analysis of the magnitude distribution of several seismic catalogues in Italy was performed. The analysis shows similar values for the q -value, in good agreement with those obtained for other seismotectonic settings [e.g. Silva et al. (2006) [2] and Vilar et al. (2007) [3]]. In particular, it is shown that the volcano seismicity is characterized by slightly lower values for q . The latter results could provide hints for further investigation in discriminating tectonic from volcanic seismicity.

© 2010 Elsevier B.V. All rights reserved.

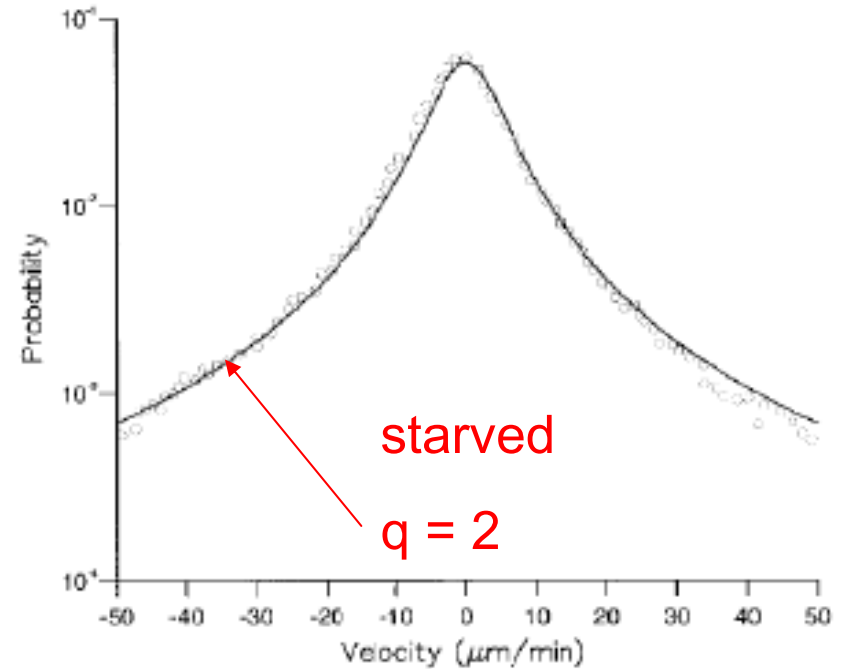
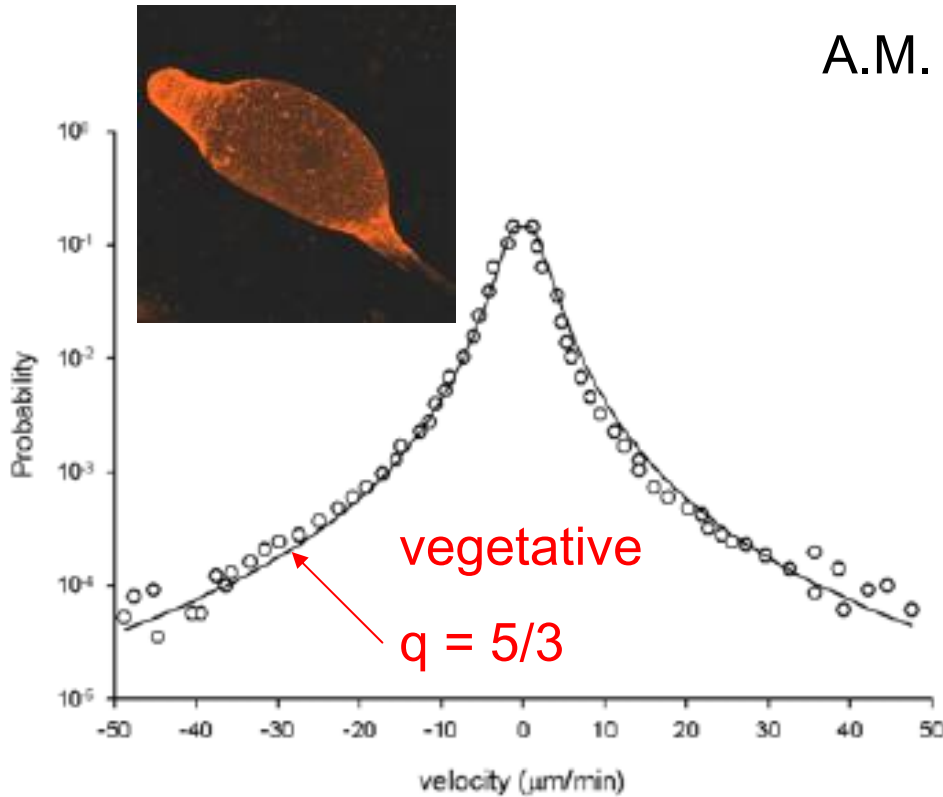


L. Telesca
Physica A **389**, 1911 (2010)

Fig. 1. Magnitude distribution and fitting with Eq. (5) for each seismic catalogue. The black continuous and dotted lines indicate the fitting curve and the 95% confidence band

Dictyostelium discoideum (cells):

A.M. Reynolds, Physica A 389, 273 (2010)



$$P(v) = \frac{\Gamma\left(\frac{\alpha+1}{2}\right)}{\sqrt{\pi} \Gamma\left(\frac{\alpha}{2}\right)} \frac{v_a^\alpha}{\left[v_a^2 + v^2\right]^{\frac{\alpha+1}{2}}} \equiv \frac{P(0)}{\left[1 + (q-1) \beta v^2\right]^{\frac{1}{q-1}}}$$

Central limit behavior of the sine-circle map at the quasi-periodic edge of chaos

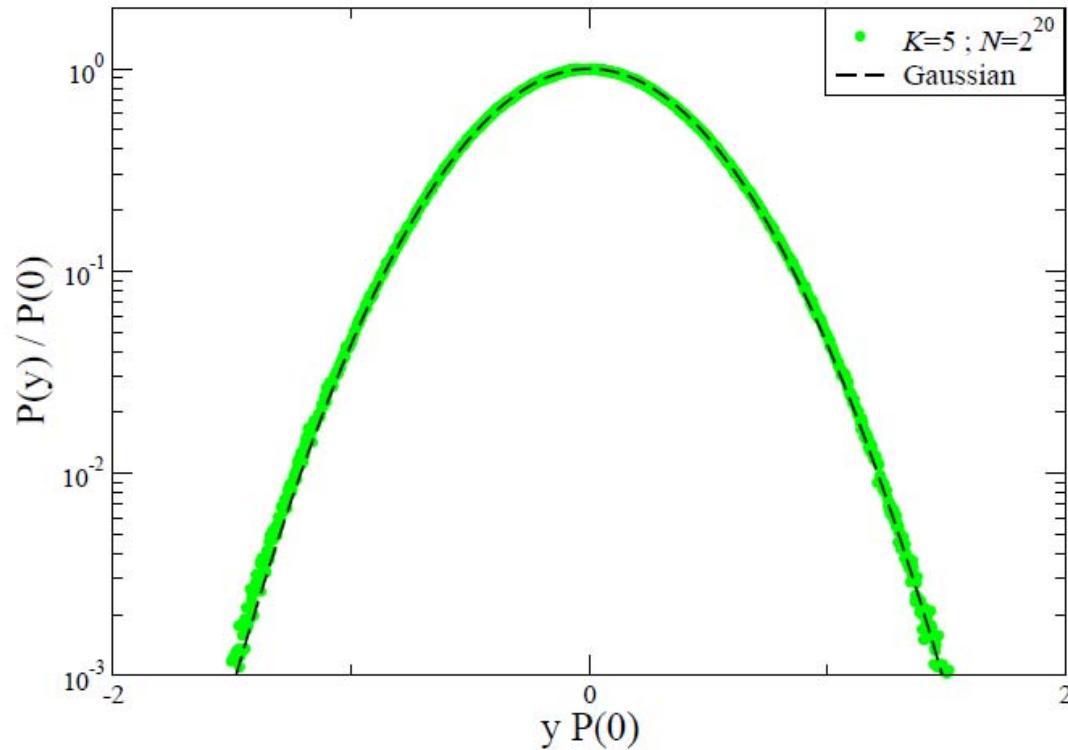


FIG. 2: Probability distribution density function of the sine-circle map for $K = 5$ and $\Omega = 0.606661063469$. Black dashed line corresponds to the Gaussian $P(y) \sim \exp(-\beta y^2)$.

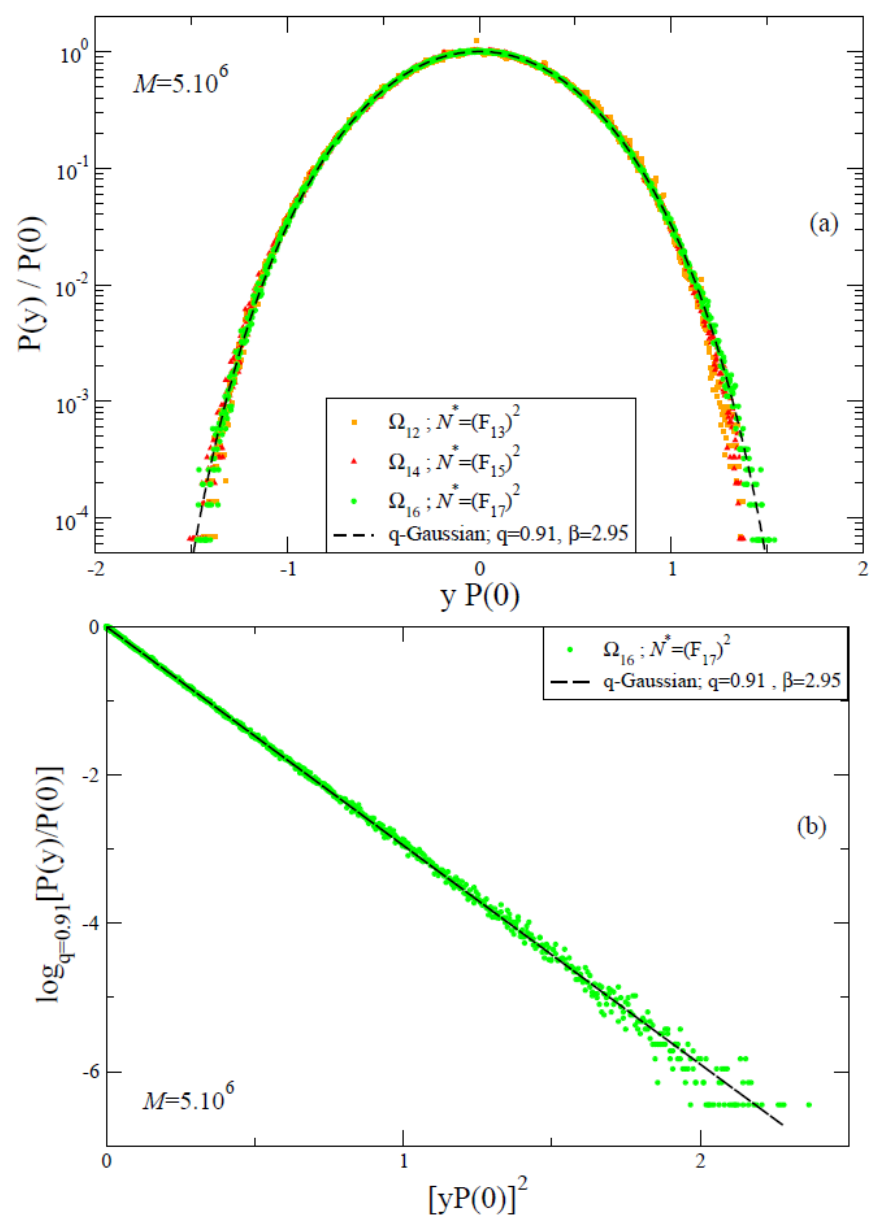


FIG. 3: (a) Probability distributions of the cases where the critical point is approached from below. (b) q -logarithmic plot of the same data for the case Ω_{16} which is the closest to the critical point that we can obtain numerically in our simulations.

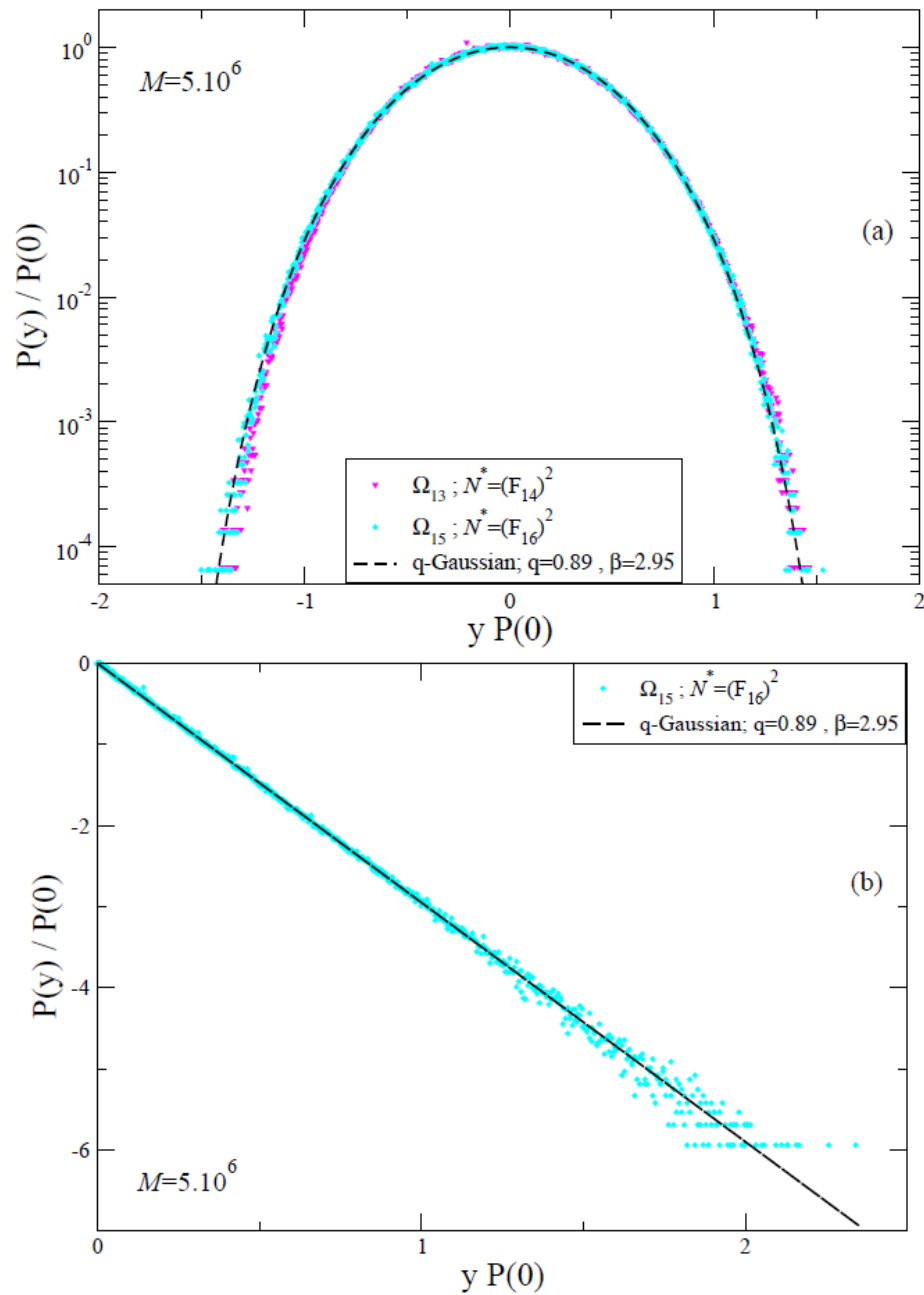
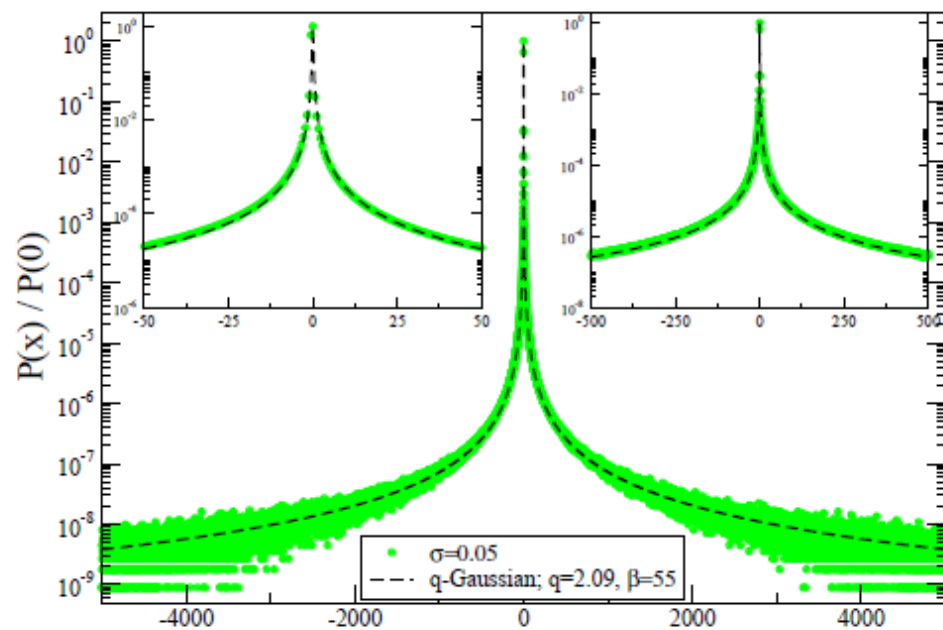
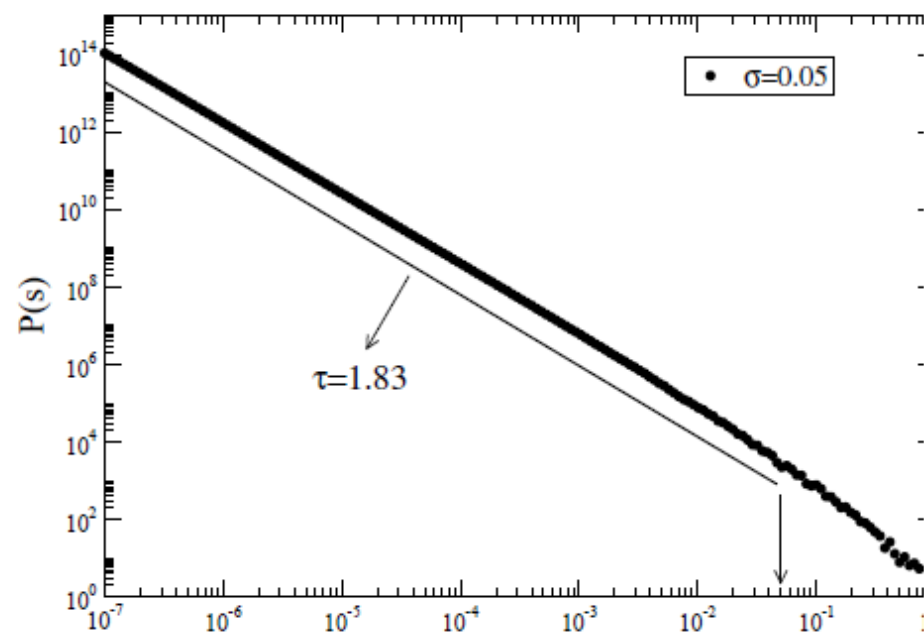
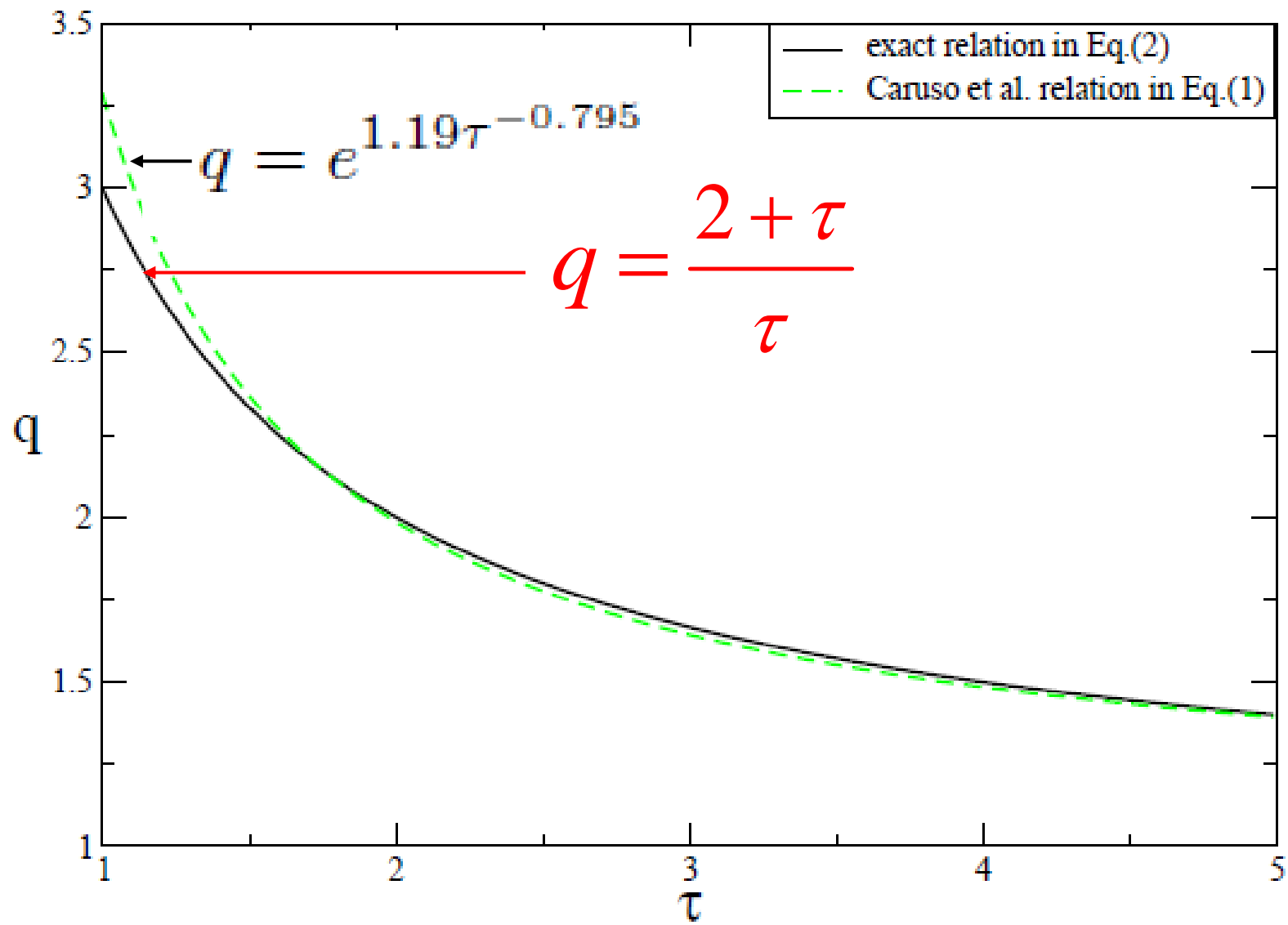


FIG. 4: (a) Probability distributions of the cases where the critical point is approached from above. (b) q -logarithmic plot of the same data for the case Ω_{15} which is the closest to the critical point that we can obtain numerically in our simulations.

Analysis of return distributions in coherent noise model



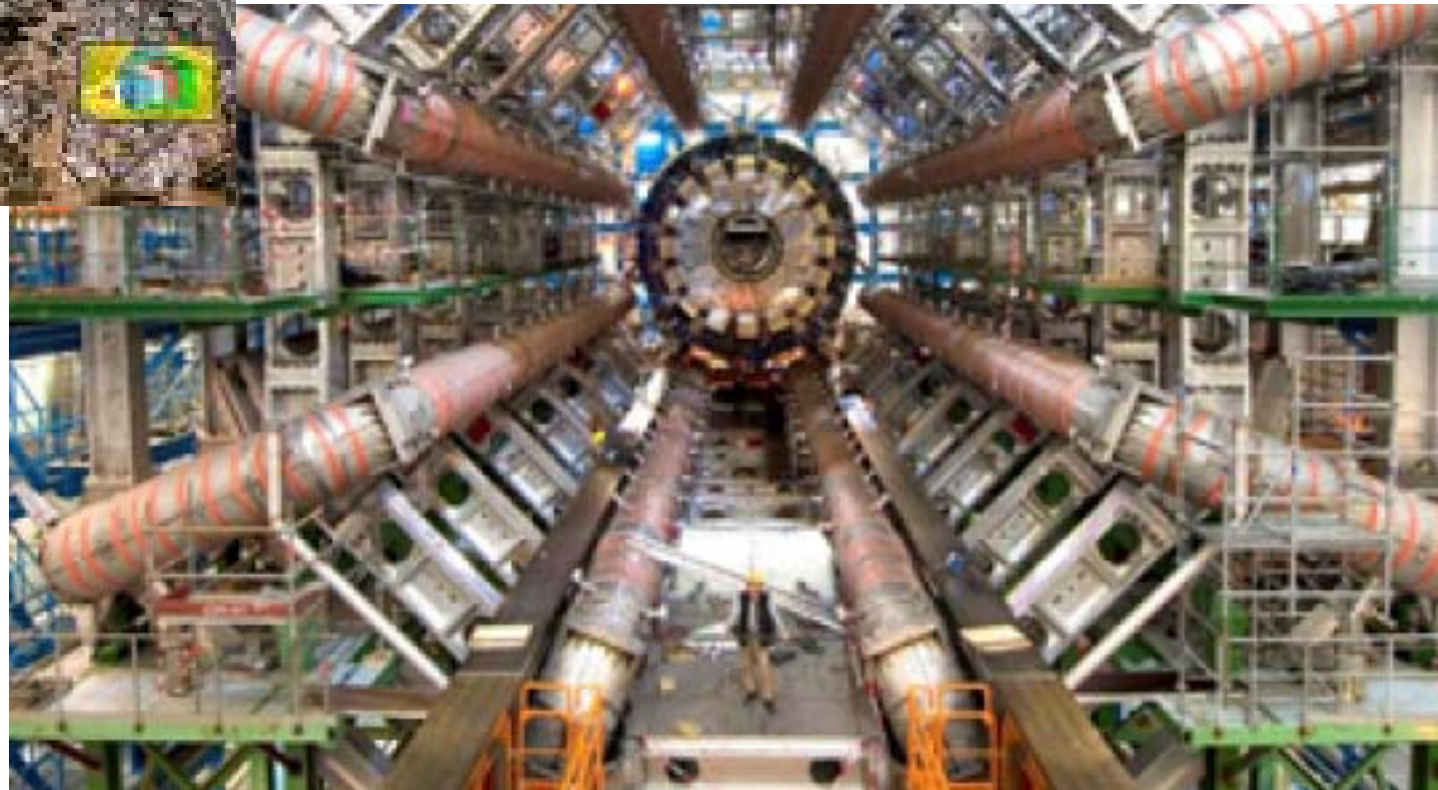
$$q = \frac{2 + \tau}{\tau}$$



LHC (Large Hadron Collider)

CMS (Compact Muon Solenoid) detector

~ 2500 scientists/engineers from 183 institutions of 38 countries



RECEIVED: February 4, 2010

ACCEPTED: February 7, 2010

PUBLISHED: February 10, 2010

Transverse-momentum and pseudorapidity distributions of charged hadrons in pp collisions at $\sqrt{s} = 0.9$ and 2.36 TeV

CMS Collaboration

ABSTRACT: Measurements of inclusive charged-hadron transverse-momentum and pseudorapidity distributions are presented for proton-proton collisions at $\sqrt{s} = 0.9$ and 2.36 TeV. The data were collected with the CMS detector during the LHC commissioning in December 2009. For non-single-diffractive interactions, the average charged-hadron transverse momentum is measured to be 0.46 ± 0.01 (stat.) ± 0.01 (syst.) GeV/c at 0.9 TeV and 0.50 ± 0.01 (stat.) ± 0.01 (syst.) GeV/c at 2.36 TeV, for pseudorapidities between -2.4 and $+2.4$. At these energies, the measured pseudorapidity densities in the central region, $dN_{\text{ch}}/d\eta|_{|\eta|<0.5}$, are 3.48 ± 0.02 (stat.) ± 0.13 (syst.) and 4.47 ± 0.04 (stat.) ± 0.16 (syst.), respectively. The results at 0.9 TeV are in agreement with previous measurements and confirm the expectation of near equal hadron production in $p\bar{p}$ and pp collisions. The results at 2.36 TeV represent the highest-energy measurements at a particle collider to date.

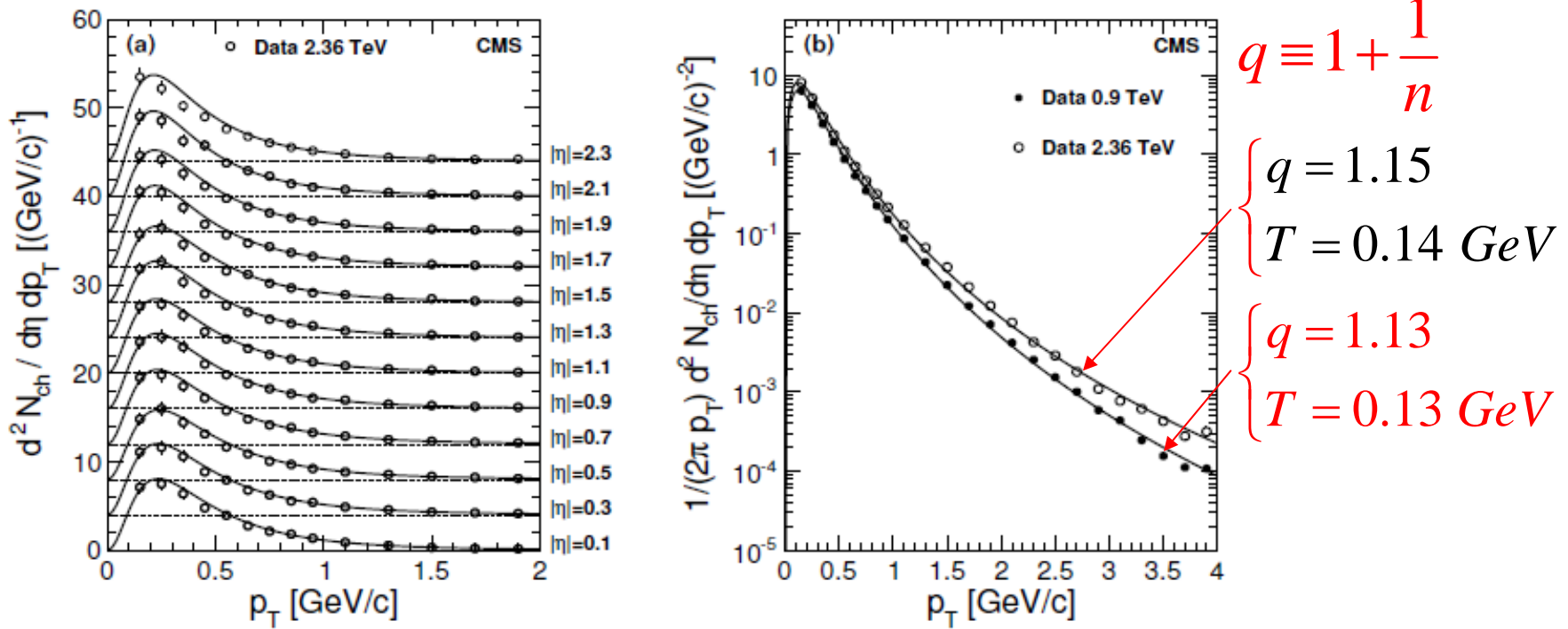


Figure 5. (a) Measured differential yield of charged hadrons in the range $|\eta| < 2.4$ in 0.2-unit-wide bins of $|\eta|$ for the 2.36 TeV data. The measured values with systematic uncertainties (symbols) and the fit functions (eq. (5.1)) are displayed. The values with increasing η are successively shifted by four units along the vertical axis. (b) Measured yield of charged hadrons for $|\eta| < 2.4$ with systematic uncertainties (symbols), fit with the empirical function (eq. (5.1)).

The yields were fit by the Tsallis function (eq. (5.1)), which empirically describes both the low- p_T exponential and the high- p_T power-law behaviours [20, 21]:

$$E \frac{d^3 N_{\text{ch}}}{dp^3} = \frac{1}{2\pi p_T} \frac{E}{p} \frac{d^2 N_{\text{ch}}}{d\eta dp_T} = C(n, T, m) \frac{dN_{\text{ch}}}{dy} \left(1 + \frac{E_T}{nT} \right)^{-n}, \quad (5.1)$$

EVIDÊNCIAS E APLICAÇÕES RECENTES:

Spin-glass

Multiple sclerosis magnetic resonance images

Interstellar turbulence

Quantum entangled spin-S chains

Ozone layer

X-ray binary systems

Seismic sequences

Motion of *Dictyostelium discoideum* (cells)

Periodic map edge of chaos

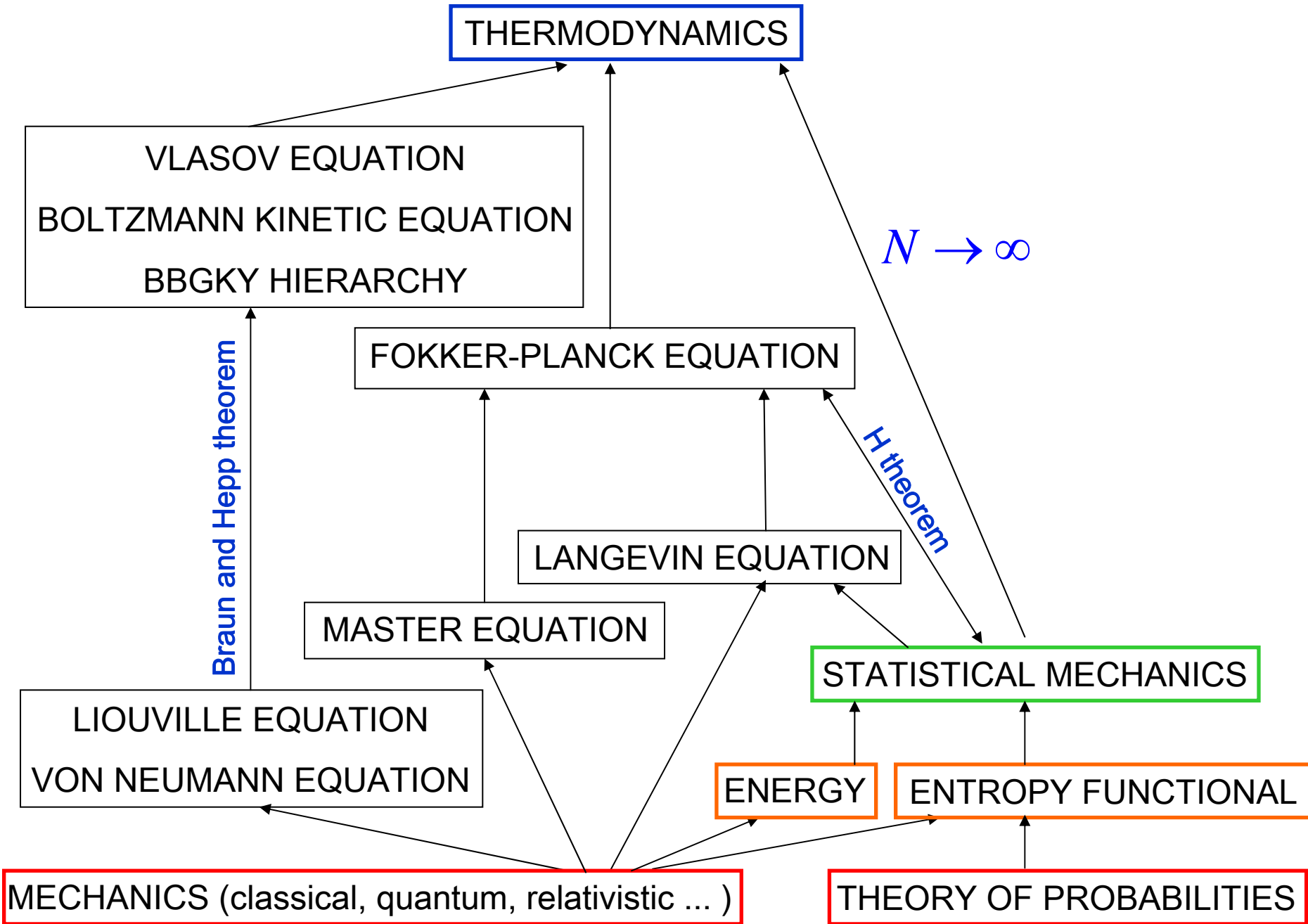
SOC in coherent noise model

LHC (CMS detector)

QUESTÕES TEÓRICAS EM CURSO:

Physical characterization of q -independence

Possibility of simultaneous $q_{entropy} \neq 1$ and $q_{limit} \neq 1$



PARADIGMATIC CASES:

BG stat mech

Nonextensive stat mech

Entropy Limit law	$S_{q_{ent}}(N) \propto N$ with $q_{ent} = 1$	$S_{q_{ent}}(N) \propto N$ with $q_{ent} \neq 1$	Other than $S_{q_{ent}}$
$e^{-\beta x^2}$ q_{lim} with $q_{lim} = 1$	independent binary variables ($\nu \rightarrow \infty$ Leibnitz-like triangle) $p_i = \frac{1}{W(N)} = \frac{1}{A\mu^N}$?	?
$e^{-\beta x^2}$ q_{lim} with $q_{lim} \neq 1$	correlated binary variables (ν – Leibnitz-like triangle) $\left(q_{lim} = 1 - \frac{1}{\nu - 1} \right)$ discretized q_{lim} – Gaussian	Nonlinear Fokker-Planck? ($q_{ent} = 2 - q_{lim} \neq 1$)	?
Other than $e^{-\beta x^2}$ q_{lim} [(q, α)-stable, HS, etc]	TGS (stretched) model MTG model MFMT model TMNT model?	TGS (restricted) ($q_{ent} = 1 - 1/d$) $p_i = \frac{1}{W(N)} = \frac{1}{BN^\rho}$ ($q_{ent} = 1 - 1/\rho$)	$p_i = \frac{1}{W(N)} = \frac{1}{C\mu^{N^\gamma}}$

$T = 0$ quantum model

$$(q_{ent} = [(9 + c^2)^{1/2} - 3] / c)$$

Strictly and asymptotically scale invariant probabilistic models of N correlated binary random variables having q -Gaussians as $N \rightarrow \infty$ limiting distributions

$$r_{N,0}^{(\nu)} = \frac{\nu \cdots (2\nu - 1)}{(N + \nu) \cdots (N + 2\nu - 1)} \quad (\nu = 1, 2, 3, \dots)$$

We prove q_{limit} -Gaussian with $q_{limit} = \frac{\nu - 2}{\nu - 1}$

					<i>$\nu \rightarrow \infty$ hence</i>
$(N = 0)$			1		$q_{limit} = 1$
$(N = 1)$		p		$1 - p$	
$(N = 2)$	p^2		$p(1 - p)$		$q_{entropy} = 1$
$(N = 3)$	p^3	$p^2(1 - p)$		$p(1 - p)^2$	$(1 - p)^3$
		\vdots		\vdots	

$(N = 0)$					1						$\nu = 1$ hence
$(N = 1)$					$\frac{1}{2}$			$\frac{1}{2}$			$q_{limit} \rightarrow -\infty$
$(N = 2)$				$\frac{1}{3}$		$\frac{1}{6}$		$\frac{1}{3}$			$q_{entropy} = 1$
$(N = 3)$			$\frac{1}{4}$		$\frac{1}{12}$		$\frac{1}{12}$		$\frac{1}{4}$		
$(N = 4)$		$\frac{1}{5}$		$\frac{1}{20}$		$\frac{1}{30}$		$\frac{1}{20}$		$\frac{1}{5}$	
$(N = 5)$	$\frac{1}{6}$		$\frac{1}{30}$		$\frac{1}{60}$		$\frac{1}{60}$		$\frac{1}{30}$		$\frac{1}{6}$

		\vdots				\vdots				\vdots	
$(N = 0)$					1						$\nu = 2$ hence
$(N = 1)$					$\frac{1}{2}$			$\frac{1}{2}$			$q_{limit} = 0$
$(N = 2)$				$\frac{3}{10}$		$\frac{1}{5}$		$\frac{3}{10}$			$q_{entropy} = 1$
$(N = 3)$			$\frac{1}{5}$		$\frac{1}{10}$		$\frac{1}{10}$		$\frac{1}{5}$		
$(N = 4)$		$\frac{1}{7}$		$\frac{2}{35}$		$\frac{3}{70}$		$\frac{2}{35}$		$\frac{1}{7}$	
$(N = 5)$	$\frac{3}{28}$		$\frac{1}{28}$		$\frac{3}{140}$		$\frac{3}{140}$		$\frac{1}{28}$		$\frac{3}{28}$
		\vdots				\vdots				\vdots	

q -GENERALIZED CENTRAL LIMIT THEOREM:

S. Umarov, C.T. and S. Steinberg, Milan J Math 76, 307 (2008)

q -Fourier transform:

$$F_q[f](\xi) \equiv \int_{-\infty}^{\infty} e_q^{ix\xi} \otimes_q f(x) dx = \int_{-\infty}^{\infty} e_q^{ix\xi} [f(x)]^{q-1} f(x) dx$$

$(q \geq 1)$

(nonlinear!)

For $q < 1$ see K.P. Nelson and S. Umarov, 0811.3777 [cs.IT]

q - GENERALIZED CENTRAL LIMIT THEOREM:

S. Umarov, C.T. and S. Steinberg, Milan J Math 76, 307 (2008)

q-independence:

Two random variables X [with density $f_X(x)$] and Y [with density $f_Y(y)$] having zero q -mean values are said q -independent if

$$F_q[X+Y](\xi) = F_q[X](\xi) \otimes_{\frac{1+q}{3-q}} F_q[Y](\xi) ,$$

i.e., if

$$\int_{-\infty}^{\infty} dz e_q^{iz\xi} \otimes_q f_{X+Y}(z) = \left[\int_{-\infty}^{\infty} dx e_q^{ix\xi} \otimes_q f_X(x) \right] \otimes_{(1+q)/(3-q)} \left[\int_{-\infty}^{\infty} dy e_q^{iy\xi} \otimes_q f_Y(y) \right] ,$$

with

$$f_{X+Y}(z) = \int_{-\infty}^{\infty} dx \int_{-\infty}^{\infty} dy h(x, y) \delta(x + y - z) = \int_{-\infty}^{\infty} dx h(x, z - x) = \int_{-\infty}^{\infty} dy h(z - y, y)$$

where $h(x, y)$ is the joint density.

q-independence means $\begin{cases} \text{independence} & \text{if } q = 1 , \text{ i.e., } h(x, y) = f_X(x) f_Y(y) \\ \text{global correlation} & \text{if } q \neq 1 , \text{ i.e., } h(x, y) \neq f_X(x) f_Y(y) \end{cases}$

On a q -Central Limit Theorem Consistent with Nonextensive Statistical Mechanics

Sabir Umarov, Constantino Tsallis and Stanly Steinberg

JOURNAL OF MATHEMATICAL PHYSICS **51**, 1 (2010)

Generalization of symmetric α -stable Lévy distributions for $q > 1$

Sabir Umarov,^{1,a)} Constantino Tsallis,^{2,3,b)} Murray Gell-Mann,^{3,c)} and
Stanly Steinberg^{4,d)}

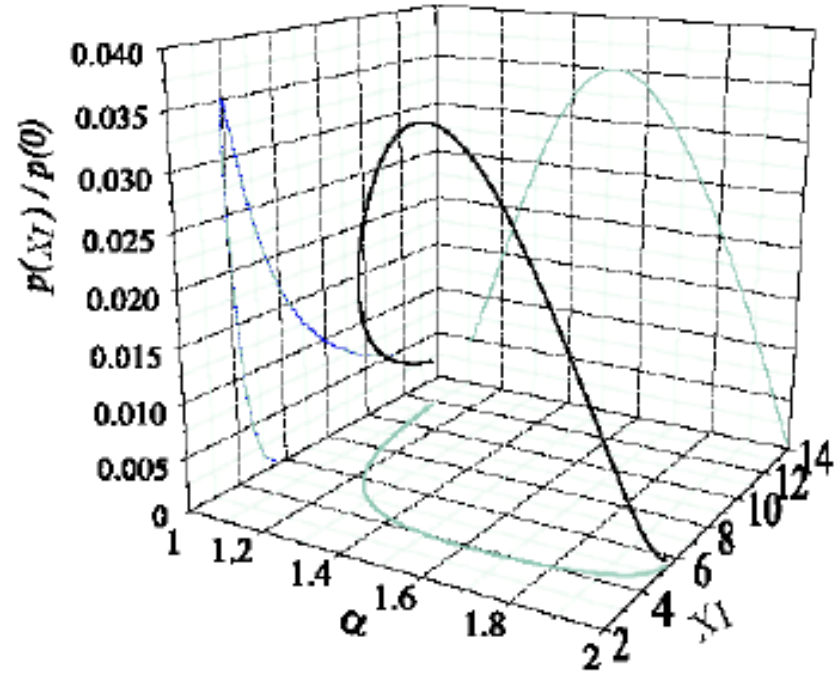
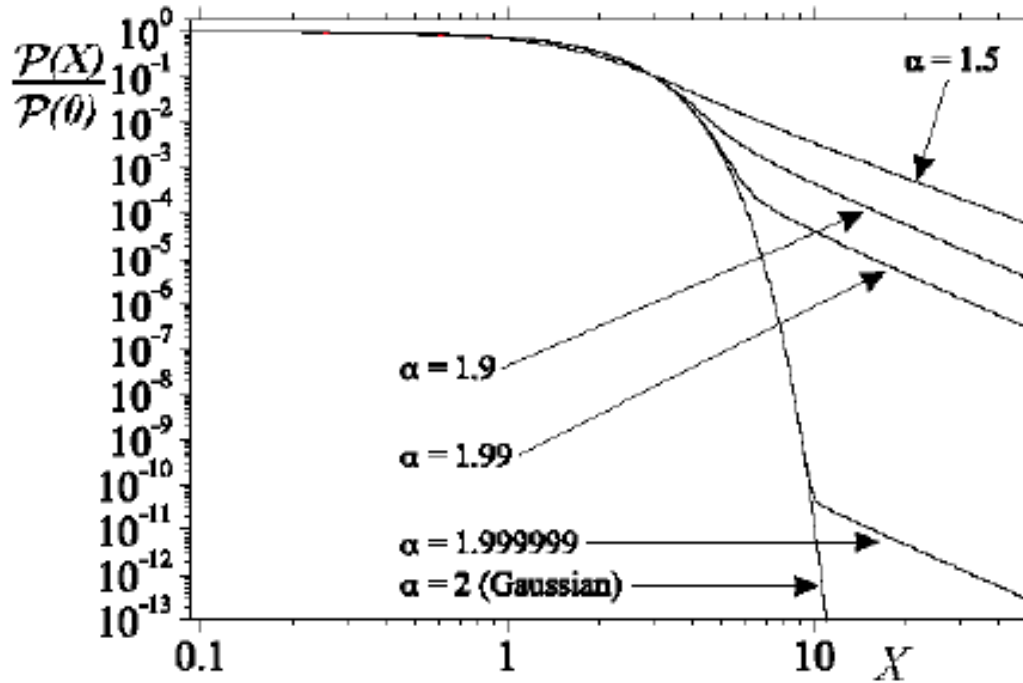
CENTRAL LIMIT THEOREM

$N^{1/[\alpha(2-q)]}$ -scaled attractor $\mathbb{F}(x)$ when summing $N \rightarrow \infty$ q -independent identical random variables

with symmetric distribution $f(x)$ with $\sigma_Q \equiv \int dx x^2 [f(x)]^Q / \int dx [f(x)]^Q$ $\left(Q \equiv 2q-1, q_1 = \frac{1+q}{3-q} \right)$

	$q=1$ [independent]	$q \neq 1$ (i.e., $Q \equiv 2q-1 \neq 1$) [globally correlated]
$\sigma_Q < \infty$ $(\alpha = 2)$	$\mathbb{F}(x) = \text{Gaussian } G(x)$, with same σ_1 of $f(x)$ Classic CLT	$\mathbb{F}(x) = G_q(x) \equiv G_{(3q_1-1)/(1+q_1)}(x)$, with same σ_Q of $f(x)$ $G_q(x) \sim \begin{cases} G(x) & \text{if } x \ll x_c(q, 2) \\ f(x) \sim C_q / x ^{2/(q-1)} & \text{if } x \gg x_c(q, 2) \end{cases}$ with $\lim_{q \rightarrow 1} x_c(q, 2) = \infty$ S. Umarov, C. T. and S. Steinberg, Milan J Math 76, 307 (2008)
$\sigma_Q \rightarrow \infty$ $(0 < \alpha < 2)$	$\mathbb{F}(x) = \text{Levy distribution } L_\alpha(x)$, with same $ x \rightarrow \infty$ behavior $L_\alpha(x) \sim \begin{cases} G(x) & \text{if } x \ll x_c(1, \alpha) \\ f(x) \sim C_\alpha / x ^{1+\alpha} & \text{if } x \gg x_c(1, \alpha) \end{cases}$ with $\lim_{\alpha \rightarrow 2} x_c(1, \alpha) = \infty$ Levy-Gnedenko CLT	$\mathbb{F}(x) = L_{q,\alpha}$, with same $ x \rightarrow \infty$ asymptotic behavior $L_{q,\alpha} \sim \begin{cases} G_{\frac{2(1-q)-\alpha(1+q)}{2(1-q)-\alpha(3-q)}, \alpha}^* (x) \sim C_{q,\alpha}^* / x ^{\frac{2(1-q)-\alpha(3-q)}{2(1-q)}} & \text{(intermediate regime)} \\ G_{\frac{2\alpha q - \alpha + 3}{\alpha + 1}, 2}^L (x) \sim C_{q,\alpha}^L / x ^{(1+\alpha)/(1+\alpha q - \alpha)} & \text{(distant regime)} \end{cases}$ S. Umarov, C. T., M. Gell-Mann and S. Steinberg J Math Phys 51 (2010), in press

LÉVY DISTRIBUTIONS:



$$L_{\alpha}(x) \sim \frac{1}{|x|^{\alpha+1}} \quad (0 < \alpha < 2; |x| \rightarrow \infty)$$

$$\lim_{\alpha \rightarrow 2} L_{\alpha}(x) \equiv G(x) \propto e^{-ax^2}$$

(q, alpha)- DISTRIBUTIONS:

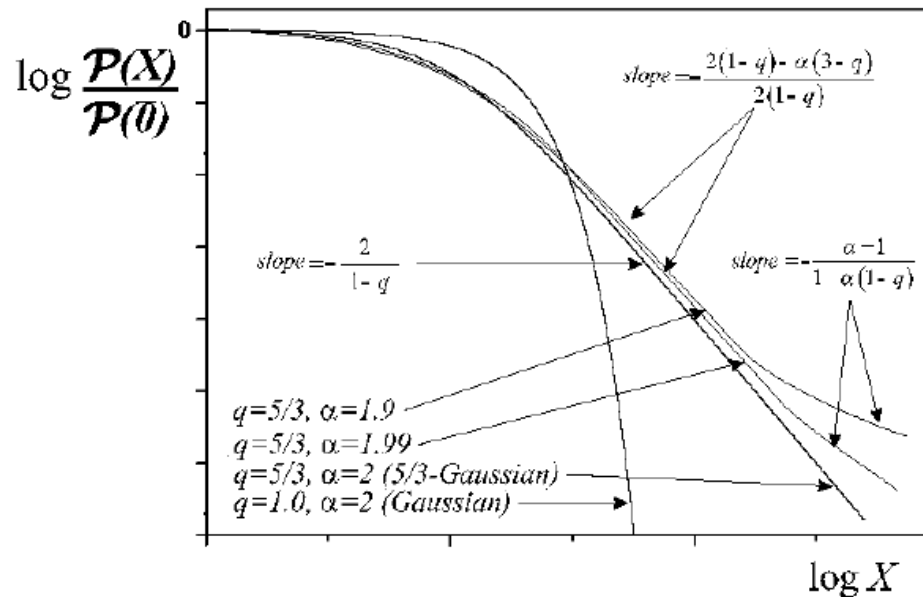


FIGURE 4. Outline of (q, α) -stable distributions for the case in which the correlation is given by $q_1 = 2$. As α of Lévy distributions approaches 2, the distributions (q, α) -stable becomes more and more similar to a $G_{\frac{5}{3}}(X)$ with an exponent $[2(1 - q) - \alpha(3 - q)] / [2(1 - q)]$. However, since $\alpha \neq 2$, for some critical value X^* , the distribution changes to another regime with a tail exponent $(\alpha + 1) / (1 + \alpha q - \alpha)$.

S.M.D. Queiros and C. T., American Institute Physics Conf. Proc. **965**, 21 (2007)

S. Umarov, C. T. and S. Steinberg, Milan J Math **76**, 307 (2008)

S. Umarov, C. T., M. Gell-Mann and S. Steinberg, J Math Phys **51** (2010), in press

ON THE PHYSICAL MEANING OF q -INDEPENDENCE

***IS (STRICT OR ASYMPTOTIC) SCALE INVARIANCE NECESSARY?
SUFFICIENT?***

q-GAUSSIAN LIMIT DISTRIBUTION? →

- 1) N compact-support continuous variables with correlation introduced through a N -variate covariance matrix **(strictly scale-invariant)** **NO!**
W. Thistleton, J.A. Marsh, K. Nelson and C. T., Cent Eur J Phys 7, 387 (2009)
[see H.J. Hilhorst and G. Schehr, J Stat Mech (2007) P06003]
- 2) N binary variables with correlation introduced through the q -product **(strictly scale-invariant)** **NO!**
L.G. Moyano, C. T. and M. Gell-Mann, Europhys Lett 73 (2006) 813
[see H.J. Hilhorst and G. Schehr, J Stat Mech (2007) P06003]
- 3) N binary variables with correlation introduced through a family of triangles generalizing the Leibnitz one **(strictly scale-invariant)** **YES!**
A. Rodriguez, V. Schwammle and C. T., J Stat Mech (2008) P09006
R. Hanel, S. Thurner and C. T., Eur. Phys. J. B 72, 263 (2009)
- 4) N -binary-discretized q -Gaussian **(asymptotically scale-invariant)** **YES!**
A. Rodriguez, V. Schwammle and C. T., J Stat Mech (2008) P09006